FIRAT UNIVERSITY
GRADUATE SCHOOL OF NATURAL AND APPLIED SCIENCES
TÜRKİYE

DETERMINATION OF BEARING CAPACITY OF OPEN ENDED STEEL SINGLE PILES

TOLAZ SALAH HAWEZ

Master's Thesis

DEPARTMENT OF CIVIL ENGINEERING
Program of
Division of Geotechnics

AUGUST 2021

FIRAT UNIVERSITY
GRADUATE SCHOOL OF NATURAL AND APPLIED SCIENCES
T Ü R K İ Y E

Department of Civil Engineering

Master's Thesis

DETERMINATION OF BEARING CAPACITY OF OPEN ENDED STEEL SINGLE PILES

Author
TOLAZ SALAH HAWEZ

Supervisor
Assoc. Prof .Dr. Hüseyin Suha AKSOY

AUGUST 2021
ELAZIG

FIRAT UNIVERSITY
GRADUATE SCHOOL OF NATURAL AND APPLIED SCIENCES
TÜRKİYE

Department of Civil Engineering

Master's Thesis

Title: Determination of Bearing Capacity of Open Ended Steel Single Piles

Author: TOLAZ SALAH HAWEZ

Submission Date: 05 July 2021

Defense Date: 16 August 2021

THESIS APPROVAL

This thesis, which was prepared according to the thesis writing rules of the Graduate School of Natural and Applied Sciences, Fırat University, was evaluated by the committee members who have signed the following signatures and was unanimously approved after the defense exam made open to the academic audience.

Signature

Supervisor: Assoc. Prof .Dr. Hüseyin Suha AKSOY — Approved
Firat University, Faculty of Engineering

Member: Assist. Prof. Dr. Gamze BILGEN — Approved
Bulent Ecevit University, Faculty of Engineering

Member: Assist. Prof. Dr. Mesut GÖR — Approved
Firat University, Faculty of Engineering

This thesis was approved by the Administrative Board of the Graduate School on

.... / .... / 20 ....

Signature

Associated Prof. Dr. Kürşat Esat ALYAMAÇ
Director of the Graduate School

DECLARATION

I hereby declare that I wrote this Master's Thesis titled " Determination of Bearing Capacity of Open Ended Steel Single Piles " in consistent with the thesis writing guide of the Graduate School of Natural and Applied Sciences, Firat University. I also declare that all information in it is correct, that I acted according to scientific ethics in producing and presenting the findings, cited all the references I used, express all institutions or organizations or persons who supported the thesis financially. I have never used the data and information I provide here in order to get a degree in any way.

16 August 2021

TOLAZ SALAH HAWEZ

PREFACE

First of all, I'd want to thank GOD for everything. for His grace and for providing me with the strength to accomplish this study, and then I'd want to thank my supervisor, Assoc.Prof.Dr. Hüseyin Suha AKSOY, for his continuous encouragement and valuable assistance throughout the study; his deep interest in this investigation and his guidance enabled me to finish this research. In addition to my supervisor, I would like to thank Mr. Nichirvan Ramadhan for his continuous help and support during this study.

I'd also like to thank my wife for her advice and talks, which helped me get through some difficult times.I would like to express my thanks to my father, mother, and brothers for helping and supporting me to complete my studies successfully.

Finally, I'd want to express my gratitude to my friends and family for their encouragement and assistance in completing my thesis successfully.

This thesis was supported by the project number MF.21.36 by Firat University Scientific Research Projects Coordination Unit (FÜBAP). The studies were carried out with the permission of the Ethics Committee 14 / 06 / 2021

TOLAZ SALAH HAWEZ
ELAZIG, 2021

TABLE OF CONTENTS

Page

Preface iv
Abstract vii
Özet viii
List of Figures ix
Lıst of Tables xii
List of Appendices xiii
Symbols and Abbreviations xiv

1. INTRODUCTION 1

1.1. Deep Foundation 1
1.2. Classification of Deep foundation 2
1.3. System of Pile foundation 2
1.4. Classification of the pile 3
1.5. Classification Based on Material and Composition 3
1.5.1. Timber pile 3
1.5.2. Concrete pile 4
1.5.3. Steel pile 4
1.5.4. FRP Pile 6
1.6. Pile Installation 7
1.6.1. Bored Pile 7
1.6.2. Driven piles 8
1.7. Open-ended pipe piles 8
1.8. Soil plugging into the pile 9
1.9. Effect of soil plug on open-ended pipe piles 10
1.10. Mechanism of Formation Soil plug and Failure of the Open-ended Pile 11
1.11. The shape of the failure surface below the pile tip 11
1.12. Method of Estimate Ultimate Bearing Capacity 12
1.13. Bearing capacity of single pile 13
1.13.1. Axial capacity piles in compression 13
1.13.2. Load transfer mechanism 13
1.14. The objective of my research 14
1.15. Outline of research 14

2. LITERATURE REVIEW 16

2.1. General 16
2.2. Historical of Pile Foundation 16
2.3. Studies on determination bearing capacity of open-ended pile 16
2.4. Studies on shear interface between sand and pile materials. 20
2.5. Studies on Skin frictional resistance of open-ended piles 21
2.6. Previous work of Finite element analysis 24

3. MATERIAL AND METHOD 26

3.1. General 26
3.2. Experimental study 26
3.3. Test tank 27
3.4. Model piles 28

3.4.1. Pile material properties 29
3.4.2. Determination of surface roughness of pile material 30
3.5. LVDTs 31
3.6. Load cell 32
3.7. Input Data Logger and Gateway. 32
3.8. Classification of the soil in using the test 33
3.9. Hand compactor 34
3.10. Determination of relative densities of this experimental 35
3.11. Static Pile Load Tests 36
3.12. Procedure determination bearing capacity of open-ended piles 36
3.13. Direct shear test for the sand 40
3.13.1. Determination of internal friction angles (ϕ) of sand 41
3.13.2. Determination skin friction angle (δ) between sand and steel piles 41
4. RESULTS AND DISCUSSION 43
4.1. General 43
4.1.1. Experimental results 43
4.2. Finite element analysis 46
4.2.1. Plaxis 3D software 47
4.2.2. Parameters of material used in Plaxis 3D 47
4.3. Results of Plaxis 3D 48
5. CONCLUSIONS 54
References 55
Appendices 58
Currıculum Vıtae

ABSTRACT

Determination of Bearing Capacity of Open Ended Steel Single Piles

TOLAZ SALAH HAWEZ

Master's Thesis

FIRAT UNIVERSITY
Graduate School of Natural and Applied Sciences

Department of Civil Engineering

August 2021, Page: xv + 65

Open-ended piles are generally used in foundation to build super structure building such as offshore engineering and the coastal that is used to transfer the load through the upper weak top soil layer to the stronger layer of subsoil strata. Open-ended piles are very important for using, due to it has smaller driving resistance compared to other types of the pile. In this study, the bearing capacity of two open-ended piles, one with a diaphragm height of 7.5cm (Type A) and the other with a 10cm (Type B) diaphragm height, is compared. The piles are tested using a special test system for soils prepared at four different relative densities (10%, 40%, 65%, 90%). The load-settlement curve for each relative density has been obtained as a result of the experiments. Experimental results indicated that bearing capacity of two piles used in the test increase with increasing relative density and the bearing capacity of open-ended pile increasing with increasing dimension of the diaphragm of the pile.

To verify the results and data which have been found by experimental study, Plaxis 3D finite element program is used in this study. The pile system was modeled by using the program and also the program has found load-settlement curve to compare with the experimental results.

Keywords: Open-ended pile, Relative density, Bearing capacity, Finite element method.

ÖZET

DETERMINATION OF BEARING CAPACITY OF OPEN ENDED STEEL SINGLE PILES

TOLAZ SALAH HAWEZ

Yüksek Lisans Tezi

FIRAT ÜNİVERSİTESİ
Fen Bilimleri Enstitüsü

İnşaat Mühendisliği Anabilim Dalı

Ağustos 2021, Sayfa: xv + 65

Açık uçlu kazıklar genellikle açık deniz ve kıyı yapılarının temellerinde, yükleri taşıma gücü düşük üst toprak tabakalarından daha sağlam alt toprak tabakalarına aktarmak için kullanılmaktadır. Açık uçlu kazıklar, diğer kazık türlerine göre daha düşük çakma direncine sahip olduğundan kullanımları önem kazanmıştır. Bu çalışmada diyafram yüksekliği 7,5 cm (Tip A) ve diyafram yüksekliği 10 cm (Tip B) olan iki açık uçlu kazığın taşıma kapasiteleri karşılaştırılmıştır. Kazıklar, dört farklı rölatif sıkılıkta (%10, %40, %65, %90) hazırlanan zeminler içerisinde deneye tabi tutulmuştur. Deneylerde her bir rölatif sıkılık için yük-oturma eğrisi elde edilmiştir. Deneysel sonuçlar, deneyde kullanılan iki kazıkta da rölatif sıkılık arttıkça taşıma kapasitesinin arttığını ve açık uçlu kazıkların taşıma kapasitesinin kazık diyafram boyunun artmasıyla arttığını göstermiştir.

Yapılan deneysel çalışma ile bulunan sonuçları ve verileri doğrulamak için Plaxis 3D sonlu elemanlar programı kullanılmıştır. Bu program kullanılarak kazık sistemi modellenmiş ve ayrıca program ile elde edilen yük-oturma eğrileri deneysel sonuçlarla karşılaştırılmıştır.

Anahtar Kelimeler: Açık uçlu kazık, Rölatif sıkılık, Taşıma gücü, Sonlu elemanlar yöntemi.

LIST OF FIGURES

Page

Figure 1.1 Classification of deep foundation. 2

Figure 1.2 Timber pile 4

Figure 1.3 Type of concrete pile. 4

Figure 1.4 The factory-applied epoxy coatings on piles 5

Figure 1.5 Cross-sectional profile of various FRP piles currently used in industry 6

Figure 1.6 The steps in bored pile 7

Figure 1.7 The steps in driven pile 8

Figure 1.8 Plug sand into the pile 9

Figure 1.9 Open-ended pile failure due to the formation of a soil plug. 11

Figure 1.10 The flat shape of failure of below piles 12

Figure 1.11 Transfer load to the piles 13

Figure 1.12 The ultimate load applied on the top pile 14

Figure 2.1 Variation of plugging soil capacity with the relative density of sand deposits [23]. 17

Figure 2.2 Variation of plugging soil capacity with ambient pressure [23]. 18

Figure 2.3 Variation of plugging soil capacity with ambient lateral stress [23]. 18

Figure 2.4 Variation of limiting stress ratio, β, with friction angles δ and φ [31] 21

Figure 2.5 There are three kinds of inner soil conditions.. (a) The soil penetration is unplugged and free; (b) Soil penetration was restricted due to a partly plugged hole; (c) There is no soil penetration since the hole is completely closed. [33] 22

Figure 2.6 Stresses acting on open pipe piles when they are(a) unplugged and (b) plugged [34]. 23

Figure 2.7 The influence of a plug on a pile's static capacity in clay [34] 23

Figure 2.8 The influence of a plug on a pile's static capacity in sand [34]. 24

Figure 3.1 all instrument for using the test 26

Figure 3.2 Model of tank 27

Figure 3.3 Model piles 29

Figure 3.4 Details of piles 30

Figure 3.5 . Determination of surface roughness. 31

Figure 3.6 Two LVDTs 31

Figure 3.7 Load cell 32

Figure 3.8 Data logger and test box 32

Figure 3.9 The sand's grain size distribution 34

Figure 3.10 Hand compactor 34

Figure 3.11 Calibration of the relative density of sand. 36
Figure 3.12 Bearing capacity determination of pile at D_r= 10% 37
Figure 3.13 Bearing capacity determination of pile at D_r = 40% 37
Figure 3.14 Bearing capacity determination of pile at Dr = 65% 38
Figure 3.15 Bearing capacity determination of pile at D_r = 90% 38
Figure 3.16 Pile installed in the model tank 39
Figure 3.17 Two LVDTs installed in the model of experiment 39
Figure 3.18 Computer machine using in the test 40
Figure 3.19 The internal friction angle of the sand corresponding to relative densities 41
Figure 3.20 Skin friction angle between sand and piles steel corresponding relative densities. 42
Figure 4.1 Load-settlement curves for both piles in Dr = 10% 43
Figure 4.2 1 Load-setelment curves for both piles in Dr = 40% 43
Figure 4.3 Load-settlement curves for both piles in Dr = 65% 44
Figure 4.4 Load-settlement curves for both piles in Dr = 90% 44
Figure 4.5 Variation between load and relative densities for both piles 45
Figure 4.6 Variation between settlement and relative densities for both pile 46
Figure 4.7 Modelling tank 46
Figure 4.8 Load-settlement curves in Plaxis 3D for pile A in Dr = 10% 48
Figure 4.9 Load-settlement curves in Plaxis 3D for pile B in Dr = 10% 48
Figure 4.10 Load-settlement curves in Plaxis 3D for pile A in Dr = 40% 49
Figure 4.11 Load-settlement curves in Plaxis 3D for pile B in Dr = 40% 49
Figure 4.12 Load-settlement curves in Plaxis 3D for pile A in Dr = 65% 50
Figure 4.13 Load-settlement curves in Plaxis 3D for pile B in Dr = 65% 50
Figure 4.14 Load-settlement curves in Plaxis 3D for pile A in Dr = 90% 51
Figure 4.15 Load-settlement curves in Plaxis 3D for pile B in Dr = 90% 51
Figure 4.16 Comparison of experimental and Paxis 3D results for pile A 52
Figure 4.17 Comparison of experimental and Paxis 3D results for pile B 53
Figure A1.1. Time-Load curve for pile A in D_r=10% 58
Figure A1.2. Time-Settlement curve for pile A in D_r=10% 58
Figure A1.3. Time-Load curve for pile A in Dr=65% 59
Figure A1.4. Time-Settlement curve for pile A in Dr=40% 59
Figure A1.5. Time-Load curve for pile A in Dr=65% 60
Figure A1.6. Time-Settlement curve for pile A in Dr=65% 60
Figure A1.7. Time-Load curve for pile A in Dr=90% 61

Figure A1.8. Time-Settlement curve for pile A in Dr=90%..61

Figure A2.1. Time-Load curve for pile B in Dr=10% 62

Figure A2.2. Time-Settlement curve for pile B in Dr=10% 62

Figure A2.3. Time-Load curve for pile B in Dr=40% 63

Figure A2.4. Time-Settlement curve for pile B in Dr=40% 63

Figure A2.5. Time-Load curve for pile B in Dr=65% 64

Figure A2.6. Time-Settlement curve for pile B in Dr=65% 65

Figure A2.7. Time-Load curve for pile B in Dr=65% 65

Figure A2.8. Time-Settlement curve for pile B in Dr=90%...65

LIST OF TABLES

Page

Table 3.1 Some researchers are using dimensions of the model tank [40]. 28

Table 3.2 Determination of model piles by some researchers [40] 29

Table 3.3 Values of Ra, $Ry$of steel pile 31

Table 3.4 Physical properties of sand 33

Table 3.5 Dry unit weight and void ratio 35

Table 3.6 The sand's internal friction angle versus the relative density of the sand [50]. 41

Table 3.7 The skin friction angle between sand and steel pile [50]. 42

Table 4.1 The ultimate bearing capacity of pile A 45

Table 4.2 The ultimate bearing capacity of pile B 45

Table 4.3 The sand parameters for both piles entered into Plaxis 3D 47

Table 4.4 The model piles parameters entered into Plaxis 3D 47

Table 4.5 The results of the comparison between experimental and Plaxis 3D were obtained. For pile A . 52

Table 4.6 The results of the comparison between experimental and Plaxis 3D were obtained. for pileB ... 52

LIST OF APPENDICES

Page

Appendix- 1: Experimental Time-Load and Time-settlement Curves of pile A 58

Appendix- 2: Experimental Time-Load and Time-settlement Curves of pile B 62

SYMBOLS AND ABBREVIATIONS

Symbols

Q_f : The pile shaft skin friction

Q_p : The end bearing resistance

PLR : The plug length ratio

IFR : Incremental filling ratio

D : Pile penetration depth

L : Length of soil plug

dD : Increase in the depth of the pile penetration

dL : Increment of soil plug length corresponding to an increment of pile penetration

$\mathrm{Q_u}$: The ultimate bearing capacity of the pile

Φ : The internal angle of friction

B : Relatively insensitive to φ

γ : Specific recovery ratio

$\mathrm{f_{so}}$: The outside unit shaft resistance of pile

$\mathrm{f_{si}}$: The inner side unit shaft resistance of pile

$\mathrm{A_o}$: The outer shaft resistance

$\mathrm{A_i}$: The inner shaft resistance.

$\mathrm{A_p}$: The cross-sectional area of the pile

$\mathrm{A_t}$: The cross-sectional area of steel tip

$\mathrm{D_{tank}}$: Diameter of model tank

$\mathrm{D_{pile}}$: Diameter of model pile

$\mathrm{R_a}$: The arithmetic mean of the absolute values of the profile divergence

$\mathrm{R_y}$: The number of the highest peak's height

$\mathrm{D_r}$: Relative density

$\mathrm{D_{10}}$: 10% of the Sand Particles Are Finer than this Size

$\mathrm{D_{30}}$: 30% of the Sand Particles Are Finer than this Size

$\mathrm{D_{50}}$: 50% of the Sand Particles Are Finer than this Size

$\mathrm{D_{60}}$: 60% of the Sand Particles Are Finer than this Size

$\mathrm{C_u}$: Uniformity coefficient

$\mathrm{C_c}$: Curvature coefficient

$\mathrm{G_s}$: Specific gravity

$\gamma_\mathrm{d}\mathrm{max}$: Maximum dry unit weight

$\gamma_\mathrm{d}\mathrm{min}$: Minimum dry unit weight

$\mathrm{e_{max}}$: Maximum void ratio

$\mathrm{e_{min}}$: Minimum void ratio

δ : Skin Friction Angle between Sand and Pile materials

$\mathrm{K's}$: Coefficient earth pressure

Abbreviations

LVDT	: Linear Variable Displacement Transducer
ASTM	: American Society for Testing and Materials
USCS	: Unified Soil Classification System
CPT	: Cone Penetration test
SPT	: Standard penetration test
FRP	: Fiber-Reinforced polymers

1. INTRODUCTION

The foundation's role is that the load from the superstructure is transferred safely to the strata without over-settlement. Whenever soil of poor bearing capacity is encountered, a decision has to be made concerning the use of a deep foundation. Assume that the cost and difficulty of the conventional foundation are high. In that case, the piled foundations are used to transmit the load to more stiff and less compressible soil or rock from a superstructure from weak-compressible strata.

The pile foundation is the branch of a structure used to transfer and carry the load of the superstructure to the bearing strata below the surface of the soil surface. Pile foundation is wide because it has low settlement and decreases failure. Piles are long and slender members that transmit the load to deeper soil or rock by poor compressible strata or water with less compressibility and strong bearing capacity, avoiding low-bearing capacity soil [1].

When the soil pile is loaded, the strata and the pile settle slightly. Since the pile settles more than the surrounding soil, frictional resistance opposite to direction of settlement is formed between the pile and the soil. This is called skin friction. During this movement, the end of the pile compresses the soil below the pile. As a result, shear and stress occur, like in the case of shallow foundations. This is known as putting an end to the resistance. The total skin friction around the pile and the end tip gives the total bearing capacity.

In general, open-ended piles are used for both offshore and on-land construction. The open-ended pile is known as a low displacement pile and affects the surrounding soil greatly. The soil tends to penetrate the inner pile and to develop a soil plug as it is inserted into the soil. During the fully plugged penetration process, the bearing capacity of the open-ended pile may be measured. In practice, the most open-ended piles are partially plugged into the sand [2].

The ultimate bearing capacity of a pile of sand depends on the relative density. In the case of open-ended pile, when the relative density of the sand increases, the bearing capacity of the pile increases, and settlement decreases.

1.1. Deep Foundation

It is one of the foundation types that transfer loads from buildings to the earth's strata. A shallow foundation has a subsurface layer that makes the deep foundation go farther down from the surface. A geotechnical engineer would propose that a shallow foundation "pile" such as for a skyscraper, be found over a shallow foundation. All of the common reasons for this are large design loads, low depth of soil, or site constraints such as property lines. Various terminology characterizes various deep foundation forms, including the pile (analogous to the pole), the pier (similar to the column), drilled shafts, and caissons.

A pile or piling is a vertical, deeply moved, or drilled structural structure into the construction site. Piles are usually carried in situ to the strata; other deep foundations are usually created by means of excavations and drilling. The terms and conditions of appointment can differ between engineering and firms. The foundations of the pile may be constructed of timber, steel, reinforced concrete, or presser composite and fiber-reinforced polymers (FRP).

1.2. Classification of Deep foundation

There are many kinds of deep foundations available. Deep foundations, on the other hand, may be generally classified as illustrated in Figure 1.1. Many variables influence the choice of a deep foundation, but constructability and cost are often the deciding ones [3].

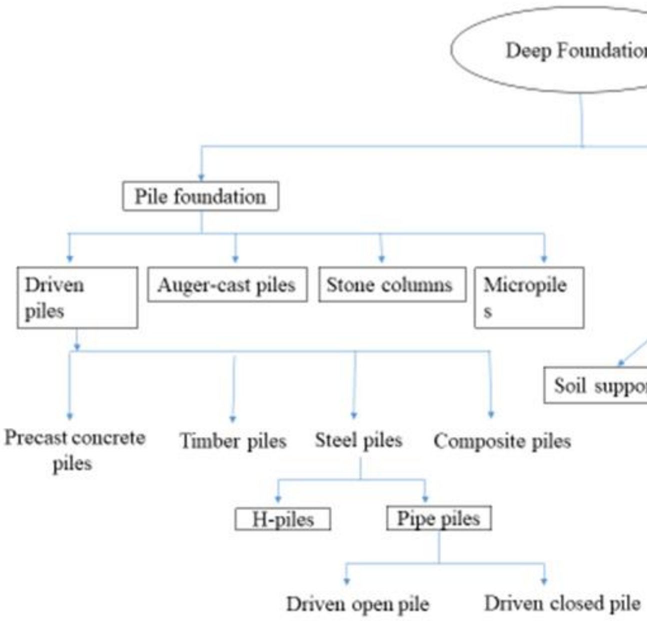

Figure 1.1 Classification of deep foundation.

1.3. System of Pile foundation

Pile foundations are preferred for compressible soils with a relatively low bearing capacity that are also susceptible to settlement problems. These foundations typically provide better solutions in comparison to shallow foundations. Piles are also preferred as foundations for problematic soils such as expansive and collapsible soils [4].They are also commonly used as foundations where stability problems due to erosion or liquefaction potential are likely.

In many scenarios, pile foundations can carry the superstructure loads safely as end bearing and friction piles. The pile shaft skin friction, $Q_{f,}$ and the end bearing resistance Q_p are derived from the combined contribution of The ultimate bearing capacity of a single pile

Several semi-empirical approaches to estimating single piles' shaft load-carrying capacity have been suggested in the literature. These techniques are drawn from many test results for field pile loads conducted on various soils. The total stress approach system is the most widely used semi-empirical method for geotechnical engineering research [5], the b method is extending the practical stress approach [6] and the l method [7].

1.4. Classification of the pile

Piles may be classified in a number of ways based on different criteria [8]:

1- Function or action.
2- Composition and material.
3- Installation.

1.5. Classification Based on Material and Composition

Piles may be classified as follows based on material and composition:

1.5.1. Timber pile

Timber piles are the oldest kind of pile foundation, having been used to carry structural loads since before recorded history began. There are simple to control, quickly lengths that are suitable, and can last a very long time under good environmental conditions. Based on their use and quality [9], many timber pile species are included shown in Figure 1.2. The piles of wood were divided into three categories piles:

1- Heavy loads of class A are piled up and transported. A minimum diameter of 356 mm is required.
2- Class B have been used to carry medium loads and have a minimum diameter of 305 to 330 mm.
3- Class C have been used for construction of structures temporary; while the whole pile is below the water table, they can be used indefinitely. The diameter should be at least 305 mm.

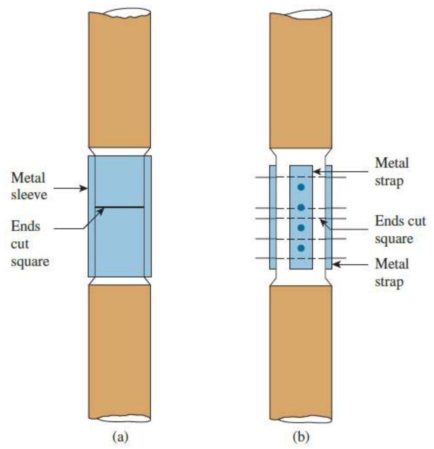

Figure 1.2 Timber pile

1.5.2. Concrete pile

Based on installation methods, tools and materials required for installation, and the names of properties, there are several forms of classifying concrete piles. This section contains information on the various forms of concrete piles, their applications, material characteristics, and material protection from impairment [9]. Displays the pile section Figure 1.3 Concrete piles are divided into three main categories:

1- Concrete piles that have been precast.
2- Concrete piles that have been Cast-in-place.
3- Concrete piles that have been Composite.

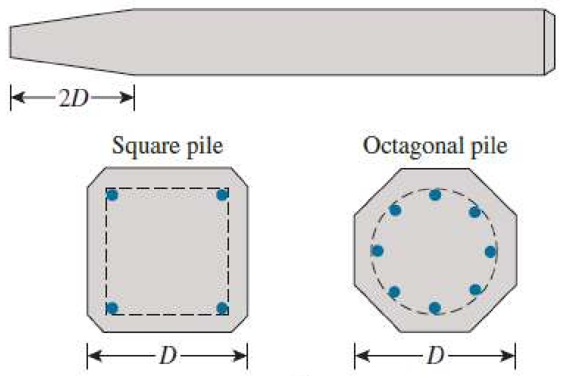

Figure 1.3 Type of concrete pile.

1.5.3. Steel pile

The steel piles are heavy, lightweight and can carry heavy loads in the deeper layers of the bearing. As splicing is relatively easy, it can be expanded to any length and can easily be reduced to any length, which allows the use of steel piles where the depth of the strata of the layer varies.

Steel piles are commonly divided into four sections: pipe-section, H-section, box section, and a tapered pile of fluted tubing (Monotubes). The most often utilized steel piles in production are pipe piles and H-section piles.

Steel piles may either be driven open or closed. Open-ended piles are less resistant to drive and may be drilled through obstacles such as rocks and bedrock.

The use of a cross-sectional area design is usually advised. Figure 1.4 shows how factory-applied epoxy coatings on piles may protect them from corrosion in certain instances. By pile driving, These are not protective coatings. readily affected. In the most corrosive areas, the concrete envelops of steel piles are frequently protected from corrosion. Typically, by driving. Here are some general steel pile facts [9]:

1- The Length between 15 m to 60 m.
2- The Load between 300 kN to 1200 kN.

Figure 1.4 The factory-applied epoxy coatings on piles

The advantage of steel pile is the following:

1- Splicing allows for simple cutoff and lengthening to the specified length
2- High-stress driving.
3- It can penetrate hard layers like thick gravel and soft rock.
4- It is capable of carrying heavy loads.

The following are disadvantage of steel piling:

1- It is relatively expensive
2- During pile driving, there is a lot of noise.
3- It has corrosion.
4- While driving, H-piles may well be destroyed or deflected from a vertical position.

5- Through difficult strata or around significant stumbling blocks.

The circular shape of the pipe piles has two main advantages:

1- Because there are no obstacles for cleaning out equipment, the soil inside the pipe may be easily removed.

2- In deep waters, the circular form reduces drag from waves and current forces.

1.5.4. FRP Pile

Composite products, especially fiber-reinforced and plastic composites, have been applied to many civil engineering industries, including geotechnical applications, in the last few decades [10]. Due to composite piling technologies' inherent benefits over conventional piling products, there has been an increase in interest in composite piling applications. The resistance mechanism to corrosive, polluted, and other hard conditions, high specific power, low weight, low maintenance, and high reliability are only a few of the small benefits composite piles have [11]. In recent years, several studies [12, 13] have defined the current state of composite piling, including pile varieties (materials), structural and geotechnical properties, drivability, and efficiency based on limited field experience. Among the benefits of FRP composite piles, they have a range of disadvantages, including higher initial prices, lower relative stiffness, lower drive performance, a lack of design standards, and a lack of an established long-term track record of usage. Because of these disadvantages, FRP piles are a compelling option for conventional piling products because of their increased durability and service life. Often, recycled plastics have been combined with steel members, or fiber-reinforced materials such as woven or pultruded fiberglass or other forms of Composite piles have been made using fiberglass reinforced polymers. Steel core piles, reinforced plastic piles, concrete-packed FRP heaps; fiberglass-pultruded piles, fiberglass-reinforced plastic piles, FRP hollow piles, and other types of piles Sheet piling made of FRP have all been recorded since 1987 [14]. Figure 1.5 displays the cross-sectional profile of different FRP piles commonly used in industry. While composite piles are becoming more popular, the majority of them have been used in marine fishing.

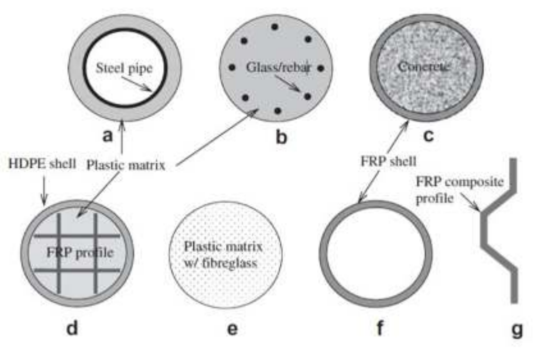

Figure 1.5 Cross-sectional profile of various FRP piles currently used in industry

1.6. Pile Installation

There are two methods of pile installation:

1- Bored pile

2- Driven pile

1.6.1. Bored Pile

Bored piles are a kind of reinforced concrete pile that is used to carry high structures with a strong vertical load. Bored piles are a type of cast-in-place concrete pile that should be cast on-site.

Boring pilling is usually done on high structures that need foundations capable of bearing thousands of tons, which are most often in unstable or hard soil conditions. A boring piling machine built specifically for soil and rock is used to cast bored piling. It may usually be drilled to a depth of 50 meters into the earth strata. Make a pile. Drilling a borehole with a certain diameter and depth would be beneficial. For the necessary cut, the borehole should have been filled with fine-aggregated concrete and strengthened with a metal frame. The bored piles are then placed and concreted on-site as a consequence. The diameter ranges from 500mm to 1500mm, while the depth ranges from 10 to 30 meters. The piles should be set up with a widening at the bottom of the borehole (a foot of pile). When there are high loads on a foundation and less compressible soils are deep-seated, this kind of bored pile is usually utilized. Figure 1.6 are shown the stepes in bored pile

Quality control is critical during the installation of a bored pile. To control the pile concreting process, each rig is outfitted with a specialized computer system. Monitoring the piles' characteristics includes depth, concrete mix pressure, concrete volume, and pile shape [15].

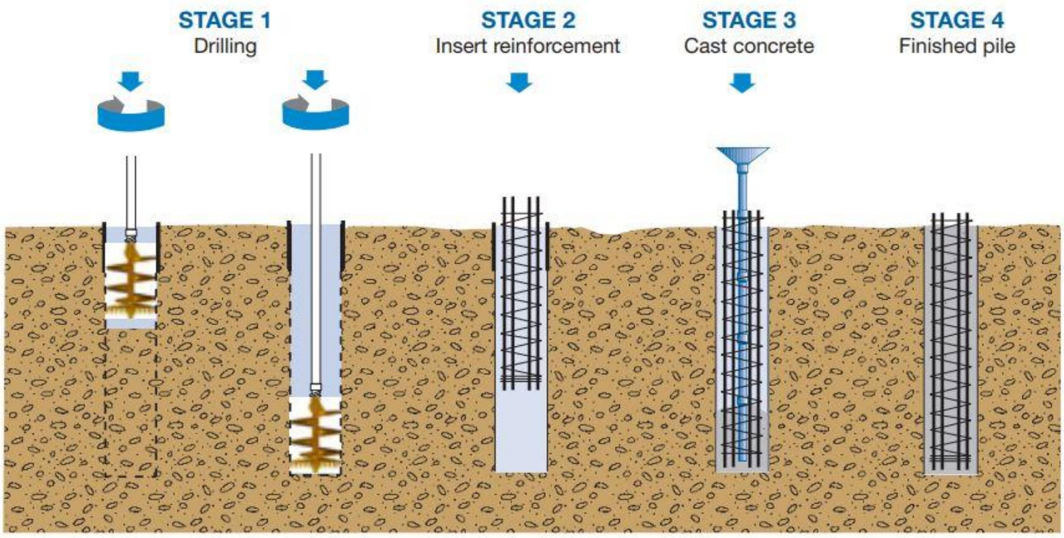

Figure 1.6 The steps in bored pile

1.6.2. Driven piles

Pile materials include wood, steel, and concrete. Precast piles are required if the piles are constructed of concrete. They may be directed at a vertical angle. Piles are driven using a pile hammer. When a pile has been driven through granular soil, the soil was compacted across the sides by the amount of soil displaced corresponding to the volume of the driven pile. The ejected parts of the soil penetrate the surrounding mass, resulting in the density of the bulk. A compaction pile is a pile that compacts the soil in its at times vicinity.

A pile's bearing capacity is increased by compacting the soil mass surrounding it. Because of its poor drainage properties, the soil surrounding a pile driven through saturated silty or cohesive soil cannot be densified. The water in the pores must be driven out before the moved soil particles may enter the empty area. Just pure water may carry the stresses developed in the soil mass next to the pile as a result of the pile's drive. This causes the creation of pore water pressure and, as a consequence, a reduction in the soil's bearing capacity. The soil next to the piles is reorganized, reducing structural strength to a degree. As a result, pushing a pile with poor drainage qualities into the soil has the direct effect of reducing its bearing strength. However, the remolded soil regains some of its lost strength over time owing to reconfiguration of the deformed particles (called thixotropy) and mass stabilization [16]. Figure 1.7 are shown the steps in driven pile.

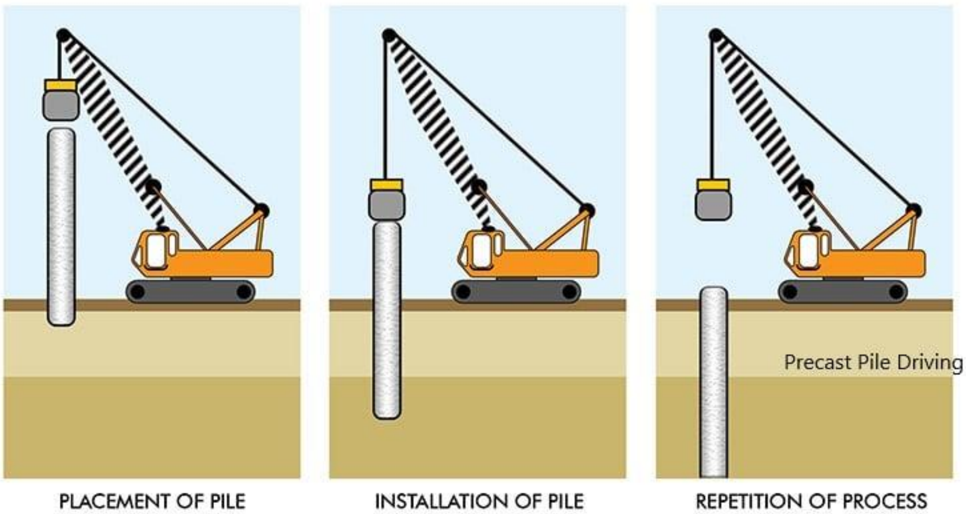

Figure 1.7 The steps in driven pile

1.7. Open-ended pipe piles

Open-ended piles that has been driven to depths of more than 50 meters have been used. A plug will form when the pile's whole cross-sectional region's internal shaft resistance exceeds resistance to end-bearing. Pre-boring the plug created inside the pile will help to reduce driving resistance. Typical diameters are about 275 mm and around 2 m with an axial load of up to 7 000 kN. Sometimes, the pile's maximum diameter depends on the capacity of the driving machine required.

The Open-end steel pile is used in the offshore wind sector to support heavy structures. When the open-end pile has been driven through strata, a soil plug may form within the pile, restricting or partially preventing the entry of additional soil. It is understood that this plugging effect largely governs open-ended piles' driving resistance and bearing capacity [2]. Figure 1.8 depicts the plug of sand into the pile.

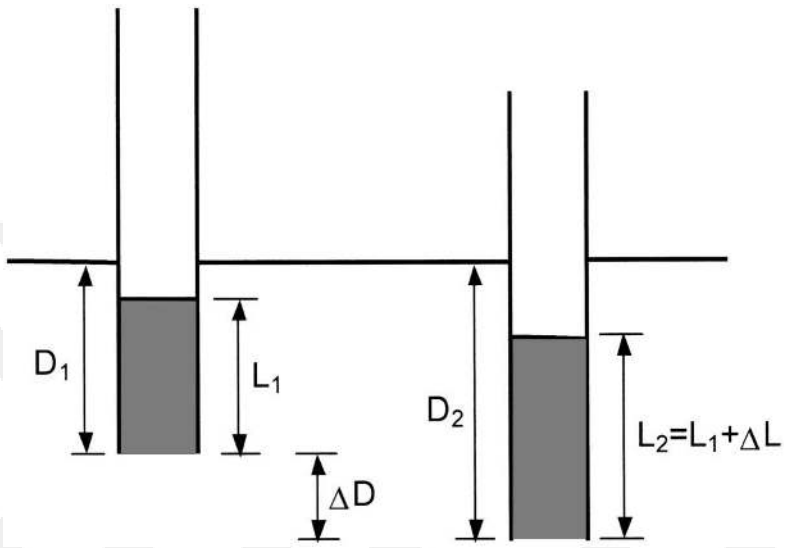

Figure 1.8 Plug sand into the pile

1.8. Soil plugging into the pile

An open-ended pile has been driven through the strata; the soil would likely get through the pile at the shallow depth during the first step of the pile driving. This is known as "completely coring" or "unplugging" behavior when the piling depth of penetration is equal to the length of the soil plug. The soil friction on the interior of the pile wall rises as the pile is driven deeper into the soil, creating a "soil plug" which prevents or partially limits more dirt from entering the pile. This is termed as "plugging," and the length of the soil plug is less than the depth of the pile penetration. Despite the fact that open-ended pipe piles' soil clogging tendency has long been known as a problem [17, 18] There are sporadic attempts that have been made to measure the percentage of soil plugs. The plug length ratio (PLR) and incremental filling ratio (IFR) are the two most often used soil plugging measurements, and are defined as follows:

$$PLR = \frac{L}{D} \qquad 1.1$$

$$IFR = \frac{dL}{dD} \qquad 1.2$$

Where:

D = pile penetration depth.

L = length of soil plug.

dD = Increase in the depth of the pile penetration

dL = lengthening of the soil plug corresponding to an increase in the depth of the pile penetration dD

Researchers have recommended using PLR to calculate the restricted unit skin friction of open-ended piles since it is a good indication of the degree of overall soil plugging [13]. A good measure of soil plugging in the calculation of end bearing values may be the IFR. It can be used to show soil plugging at the final penetration depth after the last pile drive. IFR was used to develop an equation based on model pile experiments to determine the unit end bearing value in sandy soils. Whenever the unit end bearing has been normalized to actual horizontal stress, researchers discovered that, relative density increases, and IFR decreases.

Many experiment results indicate that soil plugging is classified into two types:

1- The wedged plug zone transfers the load to the soil plug.
2- Un wedged plug zone. When the wedged plug zone is not transferring any load, a surcharge pressure exists on top of the wedged plug zone.

1.9. Effect of soil plug on open-ended pipe piles

To determine if a pile can function in plugged or unplugged mode, an open-ended pile has been required. an open-ended pile with a soil plug performs differently from a closed-ended pile driven to a comparable depth. When applied to a working load [19]. It was proposed

The open-ended ultimate bearing capacity piles have been driven by cohesive materials and may be determined by including the shaft resistance around the shaft's external diameter and the ultimate end-bearing resistance, neglecting the internal shaft resistance between the pile and the soil plug. The pile's and ultimate end-bearing with shaft resistance can be determined as though it were a closed-ended pile, although there are reduction factors of between 0.8 and 0.5, The pile's gross cross-sectional area will be used to determine end-bearing resistance. Despite having a similar ultimate resistance, the clayey soil plugs at the open-ended pile's tip will have a softer reaction than a closed-ended pile.

In granular soil, the size of the soil plug in the pipe pile has been very limited. The total of the exterior and internal shaft resistances, as well as the end bearing resistance in the pile tip's net cross-sectional area or the plug's end bearing resistance, whichever is less (Tomlinson (1994), (based on area) Observations show that the end bearing resistance of open-ended tubular piles is independent of the ultimate bearing capacity of the piles. He suggested that it should be limited to 5 MPa. This limited value may be used with a safety factor of 2.5.

1.10. Mechanism of Formation Soil plug and Failure of the Open-ended Pile

During pile penetration of the stratum based on the installation type, the soil has been inner open-ended piles when the piles are entering the strata. The soil inner piles may be created having an unique failure mode mechanism [20]. Showed Figure 1.9 as follows:

1- Figure 1.9 (a) shows the Unplugged Piles mode (coring mode). This failure mode indicates the length of the soil-created inner pile is equal to the pile's penetration depth through the strata.
2- Figure 1.9 (b) showed partially plugged piles. This failure mode indicates the length of soil created inner the pile moves to the bottom and is less than the pile's penetration depth through the strata.
3- Figure 1.9 (c) showed fully plugged piles. This failure mode indicates that the length of soil created within the pile moves downwards of the slower rate than depth of the pile penetration through the strata.

For plugged failure mechanisms, open-ended piles' end bearing capacity is determined by the soil entering the pile and forming a plug. If the soil within the pipe pile has been fully or partially plugged, the open-ended pile then behaves the same of closed-ended pipe piles.

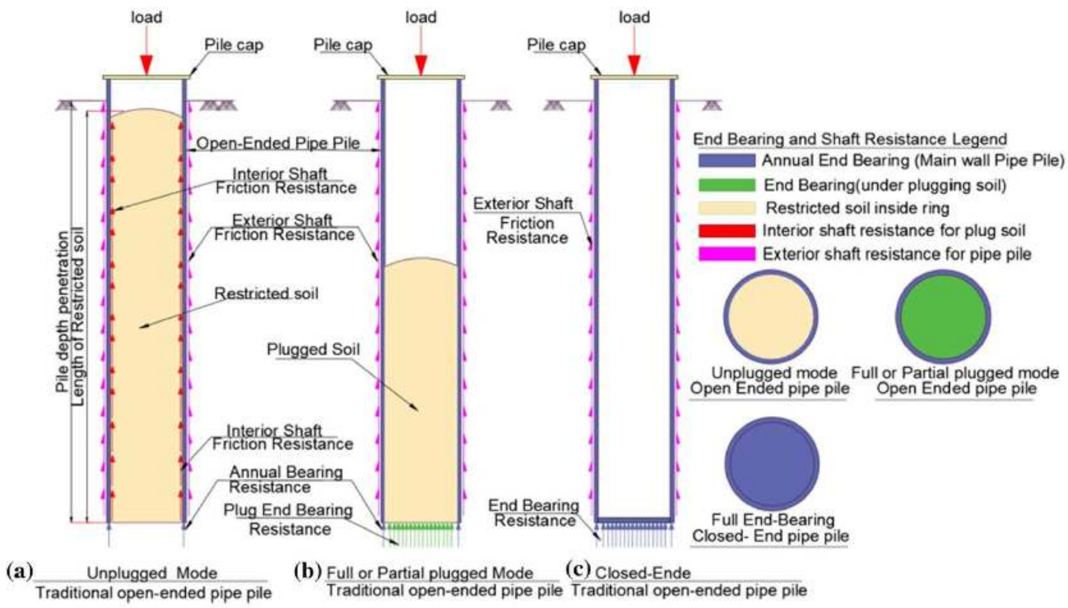

Figure 1.9 Open-ended pile failure due to the formation of a soil plug.

1.11. The shape of the failure surface below the pile tip

As when the pile penetrates the strata, the soil below the pile tip may collapse in a flat or conical pattern. The soil under the plugged pile tip is moved and extended, resulting in the formation of a cylindrical cavity. Its soil pressure has been produced by penetration resistance, and therefore, it is related to the growing cylindrical cavity. Cone-resistance has been linked to the formation of a spherical hollow under the pile tips. The area at the pile tip has the highest axial stress distribution, resulting in the highest shaft friction value amount (a few diameters above the pile tip).

The shape of the failure surface is determined by the degree of soil filling inside open-ended piles [20] Figure 1.10 shows the flat form of the failure surface shaped underneath the open-ended pile.

Figure 1.10 The flat shape of failure of below piles

1.12. Method of Estimate Ultimate Bearing Capacity

The total bearing capacity has been very complicated; it has many factors that could not be calculated in theory. The theory assumes that the soil is uniform and isotropic, but it isn't always the case. Based on plane strain conditions, all theoretical equations are obtained. The three-dimensional nature of the issue is only taken into consideration by shape effects. The soil's compression properties further complicate the problem. Therefore, experience and judgment in the application of any theory to a particular issue are essential. The skin friction Q_f depends on the pile's surface, pile installation method, and soil type. Even if the soil is homogenous across the pile's length, determining Q_f with accuracy is challenging. The issues become all the more complicated if the pile passes through soils with characteristics that change.

The following methods may find the ultimate bearing capacity, Qu, of a single vertical pile.

1- Static bearing capacity formulae are used.
2- SPT and CPT values are used.
3- Field load tests are used.
4- The dynamic method is used

1.13. Bearing capacity of single pile

A single pile's bearing capacity rises as its length and size grow. Its water table seems to have an effect on bearing capacity.

Being able to create a safe and cost-effective pile foundation and predict settlement due to soil displacement under dead weight, service load, and other conditions. The design should comply with the following requirements.

1- It should be sufficiently safe in the event of a failure; the factor of safety is determined by the structure's value as well as the strength of the soil parameters and loading.
2- The superstructure's efficiency is improved to avoid impairing its efficiency. The settlements must be compatible with adequate behavior.

1.13.1. Axial capacity piles in compression

The piles' axial capacity is generally determined by the applied loads that are transferred into the strata, as shown in Figure 1.11; they are classified as follows depending on the position of the load transmission in deep foundations:

1- End bearing piles: The load is mainly distributed at the pile's tip.
2- Frictional piles: The load had gone through the whole length of the pile. Friction between the pile material and the surrounding soil distributes
3- Combination of friction and end bearing: The load is distributed via friction both throughout the length of the pile and at the pile's tip.

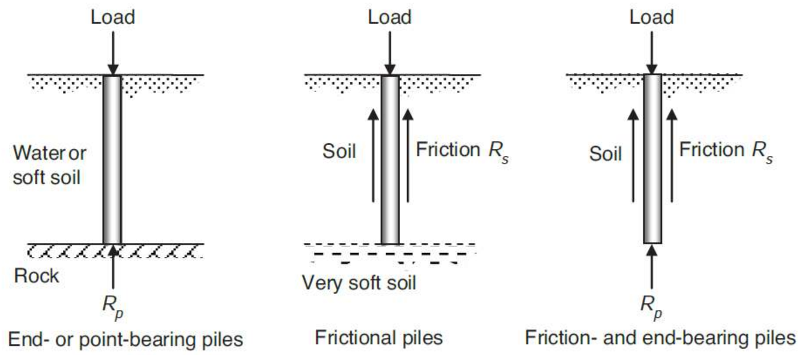

Figure 1.11 Transfer load to the piles

1.13.2. Load transfer mechanism

Figure 1.12 depicts a single pile of uniform diameter (circular or other shape) and length driven into a homogenous mass with specified physical characteristics of soil. The top of the pile is subjected to a static vertical load. It is necessary to compute the pile's ultimate bearing capacity. [15].

When the ultimate load is put to the pile's top, a portion of the load is transmitted to the soil a while of the pile's length, and the remainder is transmitted to the pile's tip. The load transferred to the soil throughout the length of the pile is known as skin friction Q*f,* and the load transferred to the pile's top is known as the point load. The total ultimate load is depicted in 1.1 by the following equation.

$$Q_u = Q_p + Q_f \quad 1.3$$

Where;

Q_u = ultimate bearing capacity of the pile

Q_p = end(point) bearing capacity of the pile

Q_f= Shaft friction resistance piles capacity

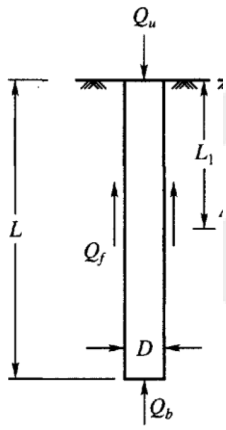

Figure 1.12 The ultimate load applied on the top pile

1.14. The objective of my research

Some of the researchers conducted an experimental study of open-ended piles, and some researchers worked on closed-ended piles, but very few researchers researched the diaphragm piles.

In this study, the load-settlement behavior of the open-ended diaphragm piles is determined, and these results are compared to the results of previous literature. Model experiments are conducted by using two diaphragm piles to determine the bearing capacity of piles. The finite element program results and experimental work results are compared.

1.15. Outline of research

The outline of research describes each chapter structure below:

Chapter one: a general description of the deep foundation. The types of piles and the open-ended piles are presented.

Chapter two: A review of the literature on the previous research's experiment on the estimated bearing capacity of open-ended piles.

Chapter three: describes the experiment's methodology and materials.

Chapter four: discusses the theoretical and experimental results. It compares results between experimental and finite elements.

Finally, chapter five presents the most important conclusions from this study and some recommendations and ideas for potential studies.

2. LITERATURE REVIEW

2.1. General

There have been many methods to determine open-ended steel piles' bearing capacity in the previous literature. There are experimental and numerical methods. This chapter provides a historical background of open-ended pile foundation bearing capacity and previous studies on open-ended piles using various methods and ideas.

2.2. Historical of Pile Foundation

Pile foundations are used as bearing capacity and load transfer devices. Villages and towns were located near rivers and lakes for communication in the initial days of civilization, for safety, and for economic purposes. As an effect, some type of piling was needed to strengthen the bearing strata. Hand-driven timber piles have been excavated and filled using sand and stones, or holes have been excavated and filled using sand and stones [21] developed pile driving machinery in the 1740s, similar to today's pile driving system. Steel piles and concrete piles have been used since the 1800s, and both have been used since the early 1900s.The development of steam and diesel-powered engines during the industrial revolution revolutionized the pile-driving mechanism. In recent years, rising housing and construction costs have pushed authorities and planning organizations to exploit land with poor soil characteristics. As a result, advanced piling and There have been developments in pile driving methods. There are several specialized installations of pile approaches available today. Previously completed work on the open-ended pile,

Several studies have researched the open-ended behavior of the pile using both experimental and finite element studies. This study will be divided into four sections:

1- Studies on the bearing capacity of an open-ended pile.
2- The shearing interface between sand and pile materials has been studied.
3- Studies on skin frictional resistance of open-ended piles
4- Studies on finite element programs.

2.3. Studies on determination bearing capacity of open-ended pile

Paik and Salgado, reported that any soil would initially penetrate the hollow pipe piles with an open-end are being driven. The soil within the pile may or may not enable more soil entry inside the pipe, based on the soil condition (dense or loose) and form (fine-grained or coarse-grained), diameter and length of the pile, and driving method. If soil reaches the pipe during the driving process, the action is said to be completing the coring, and It's more like a non-settlement pile in action. Driving was shown to be done completely plugged in, meaning that the soil develops a plug at the base of the pile, preventing additional soil entrance. A pile's load reaction would be close to that of a displacement pile If it was always driven in plug mode. In real-world situations, the action is somewhere between completely plugging and closing up. Furthermore, a pipe's action differs based on whether it is jacked or driven into the strata [2].

Szechy, stated that the amount of two-pile soil plugging and the bearing strength of varying wall thicknesses did not differ significantly (when the thickness increases, the bearing capacity of the pile increases). The thickness of the wall strongly influences the driving resistance [22].

Paik and Lee, performed a series of open-ended pipe pile calibration chamber experiments to further recognize the influence of soil quality on the load-transfer mechanism in a soil plug. While in calibration chamber, model steel piles with an outer diameter of 42.7 mm, an inner diameter of 36.5 mm, and a total of 908 mm have been used. The pile of the model was tested in a dry sand deposition of three various relative densities to measure the effect of soil conditions on the bearing capacity and behavior of an open-ended pipe pile. Model piles have been driven through the sand deposit by using hammer. The plug capacity has been plotted as a result of the stress state and relative density of sand deposits (Figure 2.1 to Figure 2.3). The relative density and lateral stress interacting with the pile tip were reported to influence the plug capacity [23].

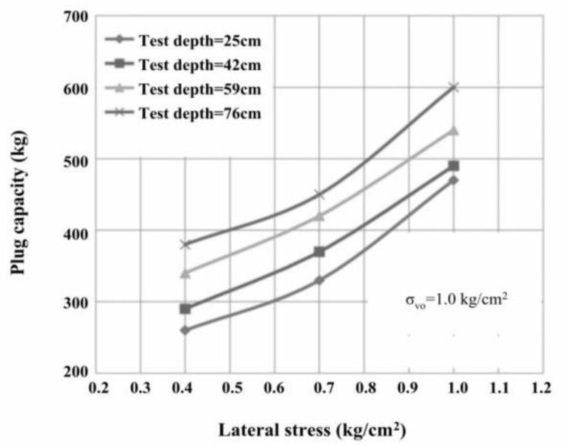

Figure 2.1 Variation of plugging soil capacity with the relative density of sand deposits [23].

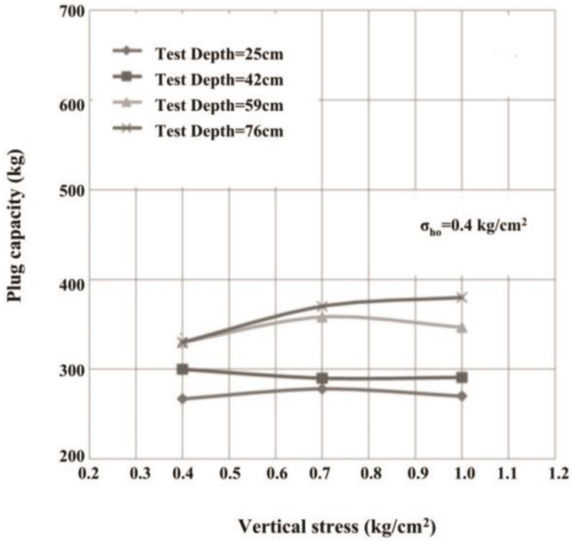

Figure 2.2 Variation of plugging soil capacity with ambient pressure [23].

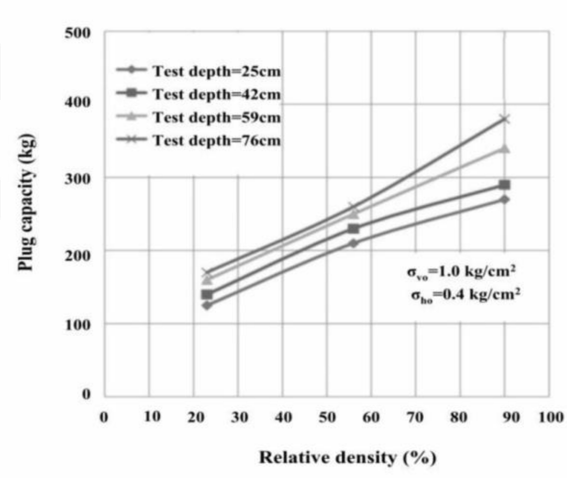

Figure 2.3 Variation of plugging soil capacity with ambient lateral stress [23].

Klos and Tejchman, carried out pile model experiments constructed of circular steel with diameters ranging from (69.9 and 128 mm), pushed to 1.0 m deep in loose and dense sand with relative densities of 41% and 70%, respectively. The level of the soil core has been seen to decrease significantly as the pile driving depth increases. "A tubular pile pushed to a depth of penetration 10 times its inner diameter would function as a solid foundation pile," it was stated [24].

Abdullah and Al – Mhaidib, The bearing potential of circular piles in sandy soil during axial loads was investigated. Open-ended piles' bearing capacity was studied as a result of piling embedment duration and length of a soil plug. Steel pipe with a 31 mm outer diameter, 27 mm inner diameter, 2 mm wall thickness, and 380 mm length has been used as a model pile. The measurements were carried out using dense sand with a unit weight of about 18.9 kN/m^3. It was suggested that the reducing factor, which was equivalent to (0.49) for sandy soil used in the analysis, a static formula may be used to determine open-ended piles' bearing capacity [25].

Paik et al, The plug in the soil that develops within the pile during pile drive affects the driving reaction and static bearing capacities of open-ended piles. Paik et al. (2003) investigated the influence of a soil plug on the static and dynamic reaction of an open-ended pile, and also the load capacity of pipe piles in general, using instrumented open- and closed-ended piles driven through sand. The open-ended pile's incremental filling ratio was computed after the soil plug duration was determined constantly throughout pile driving. By 16 percent, the open-ended pile had fewer total hammer blows than the closed-ended pile. In comparison to the closed-ended pile, the open-ended pile had a 51 percent lower limit unit shaft resistance and a 32 percent lower limit unit base 1 e N 2 resistance. The total plugging rate for the open-ended pile was around 25% of the unit resistance, and the total resistance of the friction between the soil plug and the interior surface of the open pile was 30% more than the exterior resistance of the outer shaft [2].

Lehane et al, The American Petroleum Institute's analysis in 2002, called the ICP-05, and a new methodology performed by the University of Washington known as the UWA-05, recommend different construction approaches for pile embedment sites. The most notable result of plugging into sand piles is an improvement in term resistance, with a 5 to 7-fold improvement in total base resistance of mounds that have been deployed to transferred from coring to totally plugging sandy material. In clay, closed-ended piles' base resistance allows for a much smaller proportion of overall capacity This may explain that there hasn't been any research done on the Historically, plugging had an influence on the resilience of clay piles [26].

Kikuchi et al, The plugging mechanism at the tip of open-ended axial loaded piles was identified. The motion of the iron particles combined inside the model strata with sand to form layers, extracted from described X-ray computed tomography (CT) results, determines the surrounding strata's behavior at the pile's tip. CT images of the experimental effects revealed that a wedge state is forming beneath the strata. The open-ended pile was not the same as the closed-ended pile. While the open-ended and closed-ended piles had equal penetration resistance, soil movement within the open-ended pile was limited rather than prevented, as shown by the occasional rise and During pile penetration, there is a reduction in penetration resistance [27].

Fattah et al, performed the experiment. Pipe pile plugging is a common occurrence that is not addressed properly in current design recommendations. Whenever the soil contained inside the pipe pile descends with the pile, the pile becomes plugged up. As a result, the pile is almost closed. The lateral stresses between the pile as well as the around soil are believed to be increased by plugging. As a consequence, there is greater skin friction. In 60 model pile tests, the influence of plugs on pile load carrying capacity and plug elimination was investigated. Various variables are taken into account. For example, the ratio of pile diameter to length, construction patterns in different sand densities, and the three-phase settling of the plug (50, 75 and 100%) for the plug's length. While the pile was driven, the IFR and depth of soil plugging changed, showing that the open-ended piles towards the end were partly plugged. There are two types of piles: open-ended and closed-ended. According to research, open-ended piles behave differently than closed-ended piles. The number of blows needed to drive a pile to a particular sand depth is smaller for an open-ended pile than for a closed-ended pile, according to the field test findings. Under the same property soil, It is well acknowledged that an open-ended pile needs less effort during installation than a closed-ended pile [28].

Liu et al, an open-ended pile's bearing capacity is made up of external skin frictional resistance, annular tip resistance, and plug resistance, according to the article. The difference in displacement between the pile shafts and the soil causes frictional resistance (soil plug). External and internal skin frictions, on the other hand, have separate movement processes. As the pile descends, the external skin tension develops top-down at the initial filing, and the external skin load entirely carries the operating load at the pile top that passes to the soil under the annulus of the pile. Because the pile shaft is considerably denser than the soil plug, the soils under the pile annulus are compressed more than those under the soil plug. Despite the fact that the length of the soil plug is usually constant, i.e. the pile stays plugged during static load, only a little amount of soil is driven through the pile pipe. [29].

Guo et al, according to research, the pipe wall's soil plugging behavior is highly dependent on the end bearing capability of pipe piles with an open-end. The arching develops because the inside friction between soil and piles can be inadequate to produce a completely condition of being plugged in broad diameter open-ended pipe piles, End-bearing capacity is affected following pile placement. They suggest two creatively constructed restriction plates, one with one circular hole and the other with four semi-sized circular holes, to be placed within the pipe to enhance the soil plugging operation. Using a discrete element system, the mechanical actions of soil plugs in cohesion-less soils with separate restriction plates were investigated. The numerical model was validated by comparing the results of previous laboratory-scale experiments with different pile diameters, plug length-diameter ratio, and restricted plate sizes. It is shown that the numerical simulation correctly predicts soil plug resistance and particle-scale stress transmission. Experiments and finite elements indicated that the restricted plate, particularly the four-hole restricted plate, was effective., greatly improves the arching effect. The efficacy of the restriction plate is observed to decrease as the pile diameter increases [30].

2.4. Studies on shear interface between sand and pile materials.

Randolph et al, according to research, the soil plug was subjected to a one-dimensional examination while it was drained. They took into consideration both plugged and unplugged modes of operation. If the bearing strength of the soil plug throughout its length is greater than the end bearing capacity of the plug at its tip, the pipe pile may collapse in plugged mode, but, while driving, the friction of the soil plugs induces slip relative to the pile, stopping the pile from plugging [17]. As a result, when driving in the static filling, the open-ended pile will fill up in the strata, and it will collapse as a close-ended pile. The analytical solution for plug reaction under (a) undrained and (b) drained conditions was developed by the authors. The variation of β with φ for the different ratio of tan δ / tan φ is developed (Figure 2.4), where φ is the internal angle of friction, δ is friction angle amongst soil and pile. The value of β is relatively insensitive to φ but more sensitive to the ratio tan δ / tan φ; It would be determined by the pile shaft's surface roughness and the grain size of the soil plugged material [31].

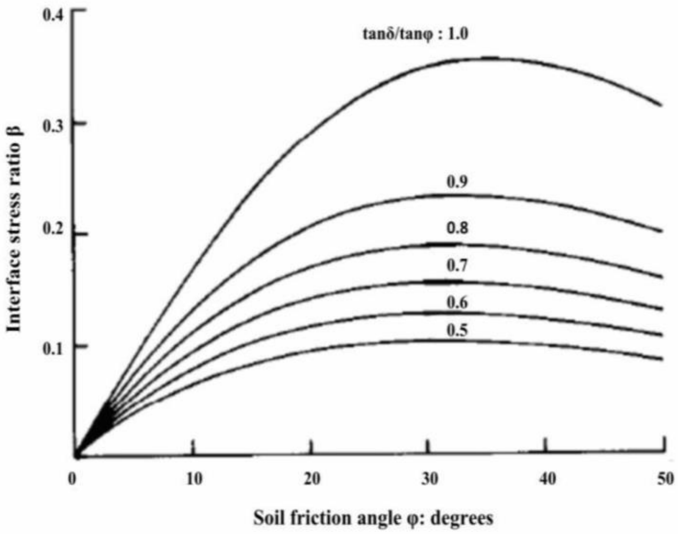

Figure 2.4 Variation of limiting stress ratio, β, with friction angles δ and φ [31].

Aksoy et al, reviewed skin friction angles between soil and steel - FRP piles. The direct shear test is using the determination of skin friction angle between steel –FRP piles. For this experiment, they used a sand-clay mixture with mixing ratios of 100:0, 80:20, 70:30, 60:40, 55:45; the results were 43°, 39.5°, 41.5°, 35°, 28° consecutively. They showed a chart determination of skin friction angle for the mentioned materials with the known value of soil's internal friction angle [32].

2.5. Studies on Skin frictional resistance of open-ended piles

Paikowsky et al, studied the phenomena of offshore pipe pile plugging and its effect on load-carrying capability (Figure.2.5). During the first stages of building, the length of soil on the pipe pile's inner side is similar to the penetration depth. Still, As penetration progresses, the soil's depth increases on the pipe pile's inner side is less than the depth of penetration due to frictional resistance. As a result, the pipe pile may be thought of as partially plugged. With further penetration, sufficient friction resistance in the pipe pile can be created, preventing any soil movement within and causing the pile to become plugged [33]Although the plugging phenomenon determines a pipe pile's load-carrying capacity, the literature's absence of data raises the following problems.:

1- Consequences of soil plugging.
2- It is also important to participate in pile-driving activities.
3- Understanding of plugging by suggesting standard plug length instead of incremental changes.

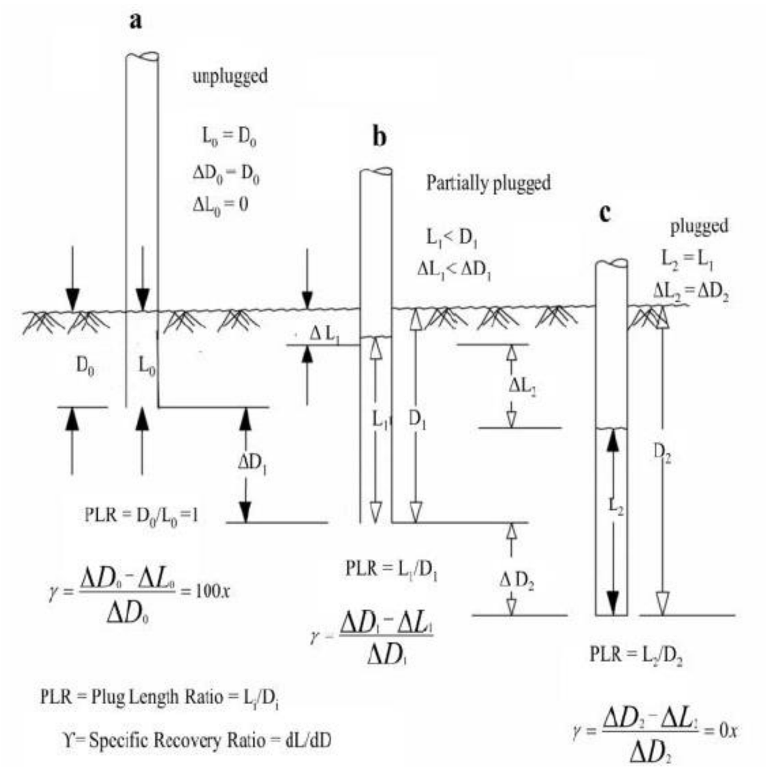

Figure 2.5 There are three kinds of inner soil conditions.. (a) The soil penetration is unplugged and free; (b) Soil penetration was restricted due to a partly plugged hole; (c) There is no soil penetration since the hole is completely closed. [33]

Paikowsky and Whitman, They have explained how a lack of understanding of soil plugging causes plugging duration to be misinterpreted as actual pile length rather than proportional pile length. As a result, wrong plug measurements are made during pile driving, and time is expected to truly understand the effects of soil plugging on pipe pile capacity. The stress acted on the pipe piles as they were plugged and unplugged, respectively [34]. (Figure 2.6) may be given:

$$Q_{unplugged} = \Sigma f_{so} A_o + \Sigma f_{si} A_i + q_p A_t \quad 2.1$$

$$Q_{plugged} = \Sigma f_{so} A_o + q_p A_p = Q_{close-ended} \quad 2.2$$

Where f_{so} is the outside unit shaft resistance of pile and f_{si} is the inner side unit shaft resistance of pile and A_o and A_i the outer shaft resistance and inner shaft resistance. A_p the cross-sectional area of the pile, A_t is the cross-sectional area of steel tip and unit end bearing capacity is the q_p.

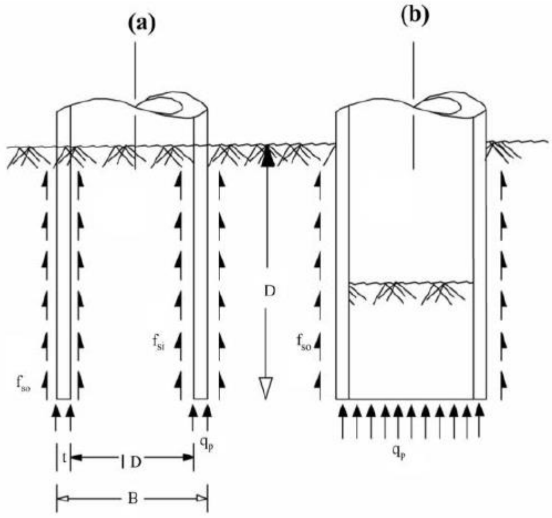

Figure 2.6 Stresses acting on open pipe piles when they are(a) unplugged and (b) plugged [34].

The point resistance moves around 25% of an ultimate load at a depth to diameter ratio of D/B= 30. Also, it is evident from Figure 2.7 and Figure 2.8. that the clay pipe pile is supposed to be plugged (i.e., when Q_{open} reaches Q_{closed}) at a depth proportion of D/B= 10-20 (approximate), whereas it takes place at D/B = 25-35, in the situation of sand. The plugging affects the performance of pipe piles in terms of load-carrying capacity.

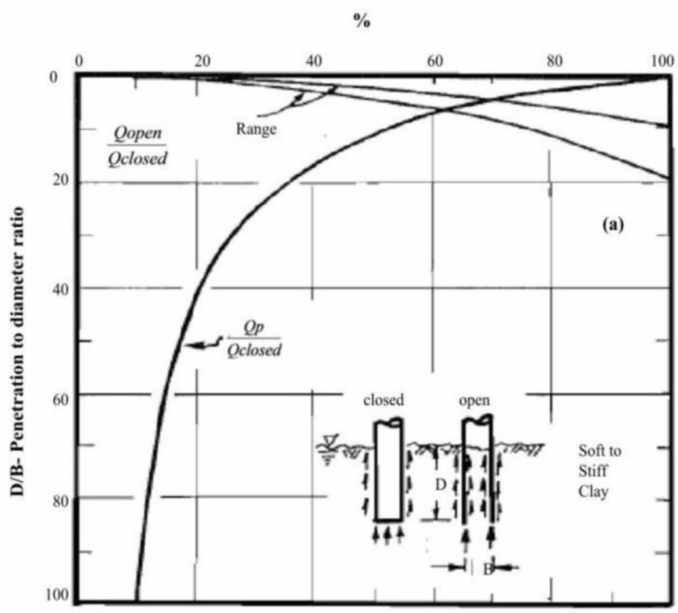

Figure 2.7 The influence of a plug on a pile's static capacity in clay [34]

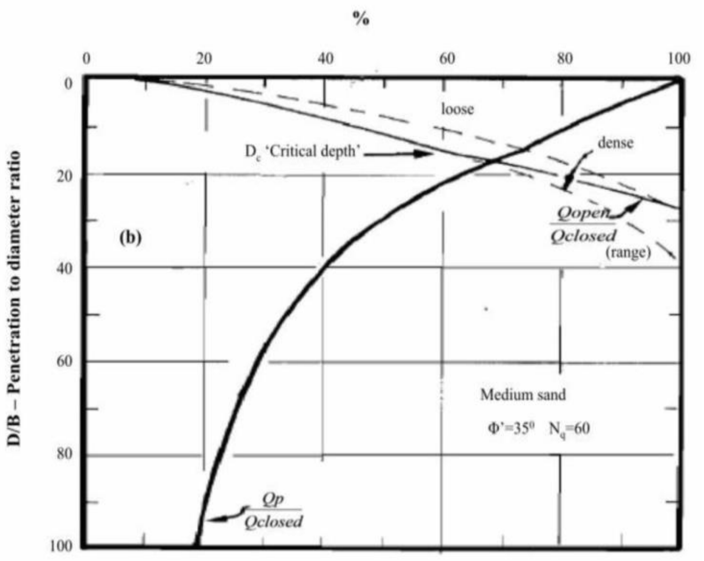

Figure 2.8 The influence of a plug on a pile's static capacity in sand [34].

Sangseom Jeong with Junyoung**,** This research looked at the effect of plugging on the capacity of open-ended piles built in sandy soil. Three instrumented piles of various diameters (508, 711.2, 914.4 mm) were used in the test to estimate the outer and inner shaft resistances operating on the piles. The pile has a double-walled structure with an instrument strain gauge on the outer and internal walls. According to field testing results, the inner shaft resistance was mainly mobilized between the pile tip and (18–34) percent of the overall plug range. Furthermore, as a measure of the IFR and pile diameter, open-ended piles' inner skin friction was proposed. Estimates may be produced using the suggested form. The degree of soil plugging and open-ended piles' inner skin friction, make it a useful tool in the engineering field [35].

2.6. Previous work of Finite element analysis

Naghibi et al, They studied the expected elastic settlement of a single friction pile under vertical loading by operating a linear finite element program on piles placed in a homogeneous soil, creating a regression model, and then developing a simple mathematical expression for calculating the elastic settlement of friction piles in a homogeneous soil. Their mathematical terminology agrees well with FE outcomes and also matches well with Randolph and Worth's theoretical solution for forecasting pile settlement. Their mathematical expression's most significant benefit is that pile duration can be conveniently measured for a fixed amount of settlement, which can then be used in pile construction and serviceability limits [36].

Kishanrao and Prasad, Plaxis 2D, a two-dimensional finite element program, was used to conduct the research, which provides a rather good method to investigate the behavior of the soil-pile interface and its response to applied axial load, researchers investigated the behavior, settlement, and load transfer mechanisms of single piles under axial loading in layered soil. They used single piles with three different slenderness ratios (L/D=7.5, 10, 12.5) embedded in two different layered soil structures, underlying sand clay and vice versa, with each pile modelled from a 2D perspective with an axis-symmetric condition. In the form of a load-settlement curve, the findings of finite element analysis were obtained. It was discovered that increasing the slenderness ratio of a single pile raises its ultimate bearing capacity, so a pile with the same slenderness ratio has a significantly higher ultimate resistance in the case of sand overlying clay than in the case of clay overlying sand [37].

Han et al, The behavior and reaction of non-settlement piles under axial stress embedded in the sand were studied. The piles used 3D finite element software (ABAQUS) to measure the pile's end-bearing capacity and shaft resistance. The study region around the pile has been finely meshed to record the development of shear bands next to the pile shaft and close to the pile's base. In the study, a large number of soil profiles and pile structure geometries were used. The study's findings showed that the earth pressure K's coefficient rises with rising sand relative density and decreasing initial confining stress. The ultimate bearing resistance of the pile tip rises as the relative density of the sand increases and the initial confining load adjacent to the pile base decreases. depending on the study findings, an equation for estimating the maximum shaft resistance and ultimate resistance of the pile base of non-settlement piles embedded in sandy soil has been proposed [38].

3. MATERIAL AND METHOD

3.1. General

This chapter will show and detail all the material properties and equipment used in this study. It also presents all experimental pile model load tests and apparatus for measuring the bearing capacity of two open-ended piles and determining the ultimate bearing capacity of the piles; it will also explain the procedure of the experiments in greater detail.

3.2. Experimental study

The tank, model piles, loading apparatus, LVDTs, sand, hand compactor, data logger, and computer are the main apparatuses of the experimental system. All parts in the figure this test were carried out in the Geotechnical Laboratory of Firat University in Turkey. Each part of this instrument is important for the experiment to determine the two open-ended piles' bearing capacity. All instruments are used in the test, as shown in Figure 3.1.

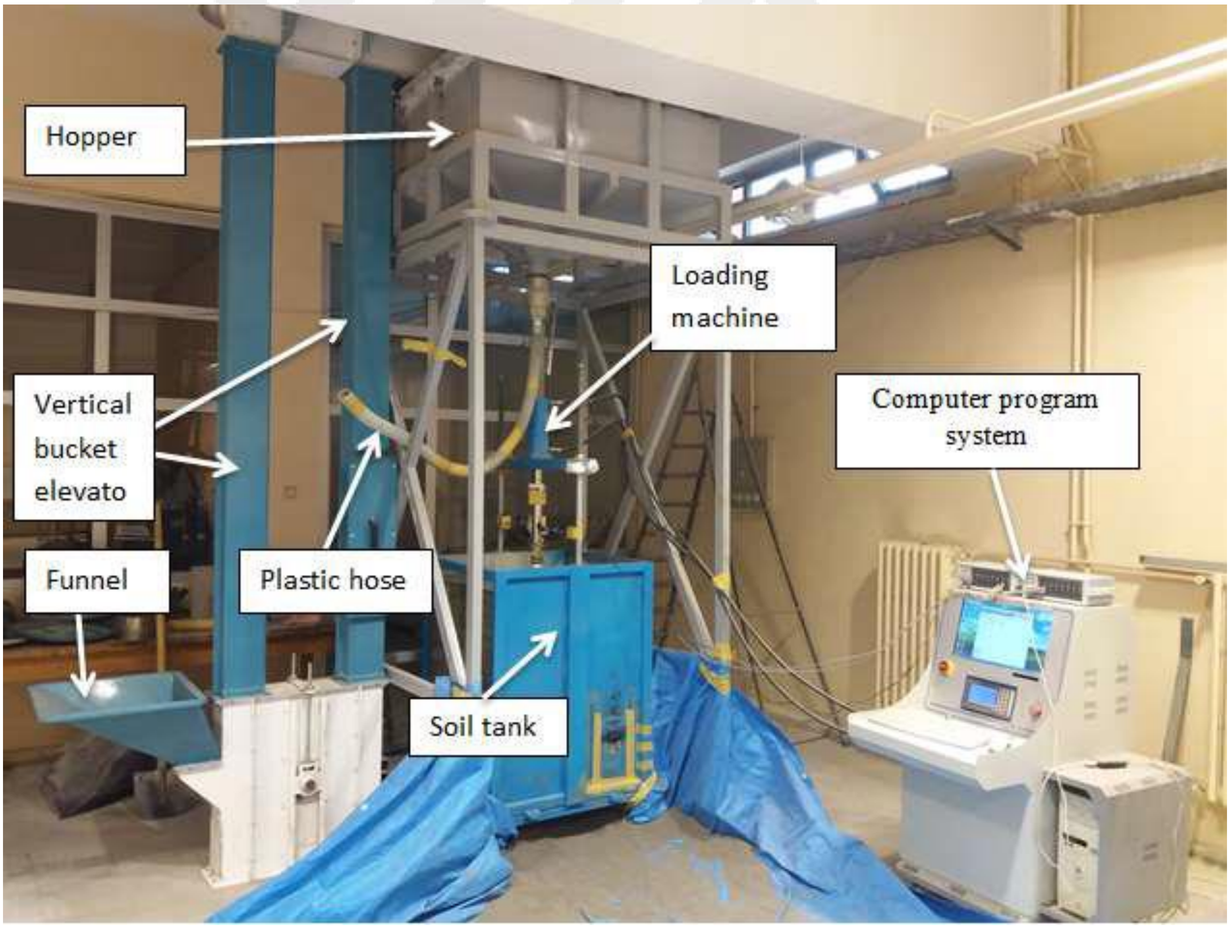

Figure 3.1 all instrument for using the test

3.3. Test tank

In this study, the tank was made of steel. The dimensions are (75 x 75 x 100 cm). The tank's dimensions are determined by several researchers, as shown in Table 3.1 The steel circular steel pipe connected to the tank is used to carry the hydraulic jack. The hydraulic jack is operated mechanically and electrically and has a power of 30 kN. The hydraulic jack used to the axial load of the top pile to embedded in the sand. The bottom of the model tank has a gate that is used to empty the sand during the testing process depicted in Figure 3.2.

The tank is the main part of the experiment that is performed the test putting the sand by the plastic pipe. The plastic pipe was used to drop the sand into the tank when the sand is transferred and stored at the top funnel, this plastic pipe connecting the funnel. The funnel sand is coming to the bunch elevator that is used to transfer sand to the funnel. Before it is starting, the test must be the classification of the soil.

Bolton et al, proposed two guidance lines to avoid the effect of boundary and scale on the model piles' bearing capacity. According to them, the ratio of the soil tank diameter to the diameter of the model pile (D_{tank}/D_{pile}) must be greater than 8, and the diameter model pile must be greater than the average of the soil particles diameter (20*D50). (D_{tank}/D_{pile}) = 15, which is higher than 8, and model pile diameter = 50 mm, which is higher than (20*D50=9.5 mm) in this study [39].

Figure 3.2 Model of tank

Table 3.1 Some researchers are using dimensions of the model tank [40].

Reference	Soil model tank diameter (mm)
Vesic (1963, 1964)	2450
Hanna et al (1973) Tan et al (1974)	610 x 610
Das et al. (1977)	475 x 610
Chaudhuri et al (1983)	1100
Kerisel et al (1964)	6400
Robinsky and Morrison (1964)	501 x 711
Shin et al. (1993)	457 x 457
Al-Mhaidib (2001)	450
Mayoral et al. (2005)	510
Nanda and Patra (2011)	750
Present Study	750x750

3.4. Model piles

In this study have two model open-ended steel pile. The length of piles is 600 mm, and the exterior diameter is 50 mm. The piles are different dimensions one pile has a 7.5 cm diaphragm from the tip of the pile, and it has a 10 cm diaphragm. In order to the exterior diameter is 50 mm also interior diameter is 46.2 mm Shows Figure 3.3, those dimensions are according to the several types of research to present the length of model pile shows in Table 3.2

Piles are installed in the center of the tank, but the bottom of the pile is 400 mm far from the bottom of the tank because the tip of the pile near the tank bottom may affect the result. According to foundation design, the stress due to applied load on the foundation may affect depth (1.5B, 2B), where B is the short dimension. In this study, the depth between the bottom piles and the bottom of the tank is 400 mm (400 mm > 2B).

Figure 3.3 Model piles

Table 3.2 Determination of model piles by some researchers [40]

Reference	Model pile diameter (mm)	Soil model tank to model pile diameter ratio
Vesic (1963, 1964)	50.8 - 171.5	14.29 - 48.23
Hanna et al (1973) Tan et al (1974)	15.7 - 38	16.05 – 38.85
Das et al. (1977)	25.4	18.7
Chaudhuri and Symons (1983)	25.4 - 50	22 – 43.31
Kerisel (1964)	40 - 320	20 - 160
Robinsky and Morrison (1964)	20.5 - 37.5	24.44 – 13.36
Shin et al. (1993)	25.4	17.99
Al-Mhaidib (2001)	30	15
Mayoral et al. (2005)	51	10
Nanda and Patra (2011)	32	23.44
Present Study	50	15

3.4.1. Pile material properties

In this study, we have two open-ended piles made of the A36 steel. The piles are different dimensions that one pile has 7.5 cm diaphragm from the tip of the pile (Pile A), and another has 10 cm diaphragm from the tip (Pile B), details of piles shown in Figure 3.4, in the that piles are 500 mm embedded in the sand during the experiment.

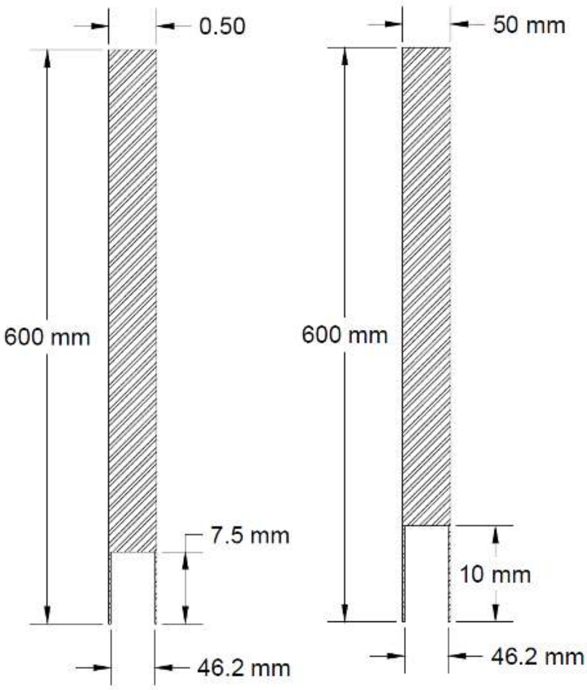

Figure 3.4 Details of piles

3.4.2. Determination of surface roughness of pile material

Roughness has been an important parameter to consider when deciding if a surface is appropriate for a given function. Rough surfaces may also wear out more easily than smoother surfaces. Unrefined products are usually more resistant to corrosion and cracks, but they may still help with adhesion.

Mutitoyo SJ-201 surface roughness tester was used to measure the steel materials' surface roughness. Figure 3.5 shows the determination of surface roughness parameters. The mean surface roughness parameters developed from the measurements performed are shown in Table 3.3.

The surface roughness parameters (R_a and R_y) are estimated using the following equations:

$$R_a = \frac{1}{N} \sum_{i=1}^{N} /Yi/ \quad 3.1$$

$$R_y = Y_p + Y_v \quad 3.2$$

Where;

R_a = The arithmetic mean of the absolute values of the profile divergence (Y_i) of the estimated distance from the mean line.

R_y= The number of the highest peak's height (Y_p) and the lowest valley's depth (Y_v) of the estimated distance from the mean line

Table 3.3 Values of R_a, $R_y$of steel pile

Model pile	R_y	R_a
Steel	3.43	0.55

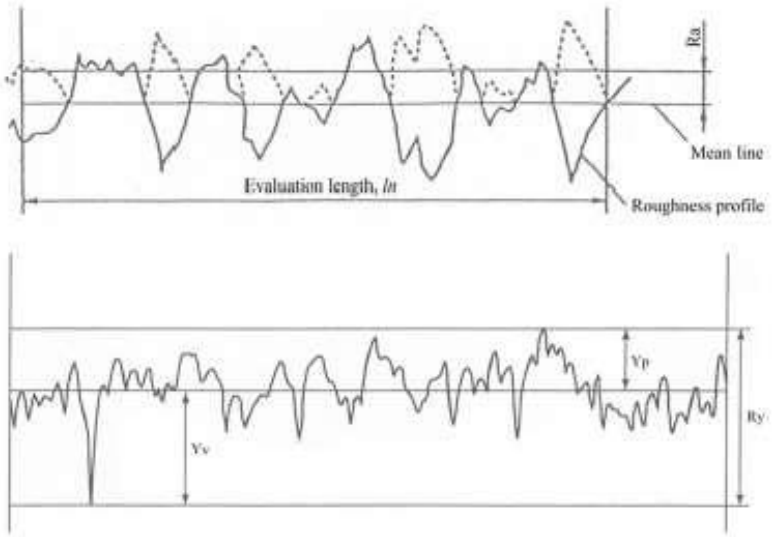

Figure 3.5 . Determination of surface roughness.

3.5. LVDTs

LVDT is an OPKON manufactured linear transformer differential, which can estimate settlements up to 150 mm, which were used to estimate the model pile's settlement due to the vertical loading shows in Figure 3.6. The pile's settlement was determined as the average of the two measurements.

Figure 3.6 Two LVDTs

3.6. Load cell

The main part of the test is the S-type Keli load cell, with the capacity to determine pile loads of 5 tons attached between the pile and the hydraulic jack as shown in Figure 3.7.After computer programming is registered, the data logger transfers load data.

Figure 3.7 Load cell

3.7. Input Data Logger and Gateway.

The values determined by the 5 tons' capacity S-type Keli load cell and the LVDTs were transmitted to the computer using a TDG-branded data logger of the Ai8b platform's eight-channel input and the same brand's RS-485 model gateway, as shown in Figure 3.8.

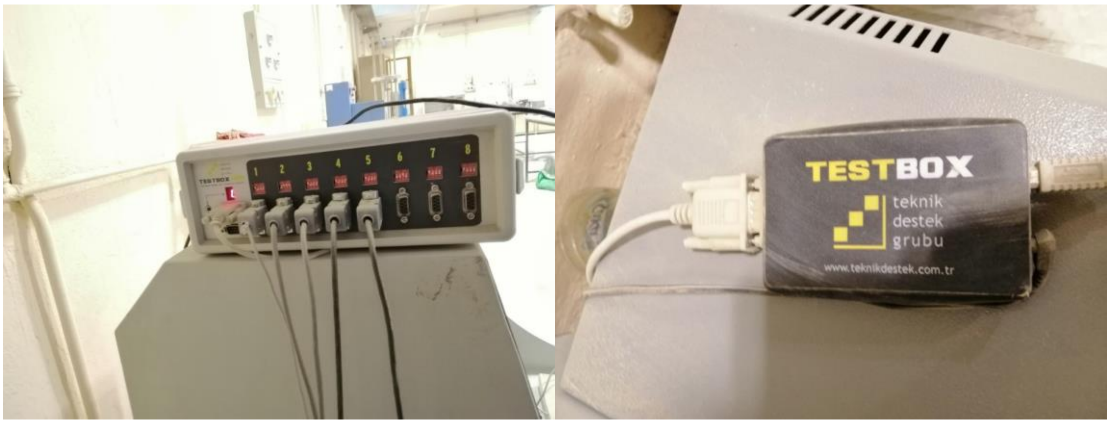

Figure 3.8 Data logger and test box

3.8. Classification of the soil in using the test

In this study, soil was uniformly classified as river sand brought from the Murat River in Turkey's Elazığ. The sand has been cleaned and oven-dried, and sieved by passing a 1 mm opening sieve and kept on sieve #200 (0.075 mm). The sieve analyses and specific gravity tests were conducted depending on standards (ASTM D422-63 and ASTM D854-14) [41, 42]. The relative density of the sand had been estimated, according to (ASTM D4254-16) [43]. The sand is categorized as poorly graded sand (SP) (USCS), which refers to the Unified Soil Classification System according to ASTM D2166 [44]. Figure 3.9 indicates the sand's grain size distribution curve. The physical characteristics of sand are recommended in Table 3.4 below.

Table 3.4 Physical properties of sand

Property	Value
Effective size, D_{10}, D_{30},D_{50}, D_{60} (mm)	0.19, 0.325, 0.475, 0.55
Uniformity coefficient, C_u	2.895
Curvature coefficient, C_c	0.980
Soil classification (USCS)	SP
Specific gravity, G_s	2.77
Maximum dry unit weight, γ_d (max.) kN/m^3	17.66
Minimum dry unit weight, γ_d (min.) kN/m^3	14.32
Maximum void ratio, e_{max}	0.898
Minimum void ratio, e_{min}	0.539
Maximum – Minimum grain size, D_{max}-D_{min} (mm)	1 - 0.074

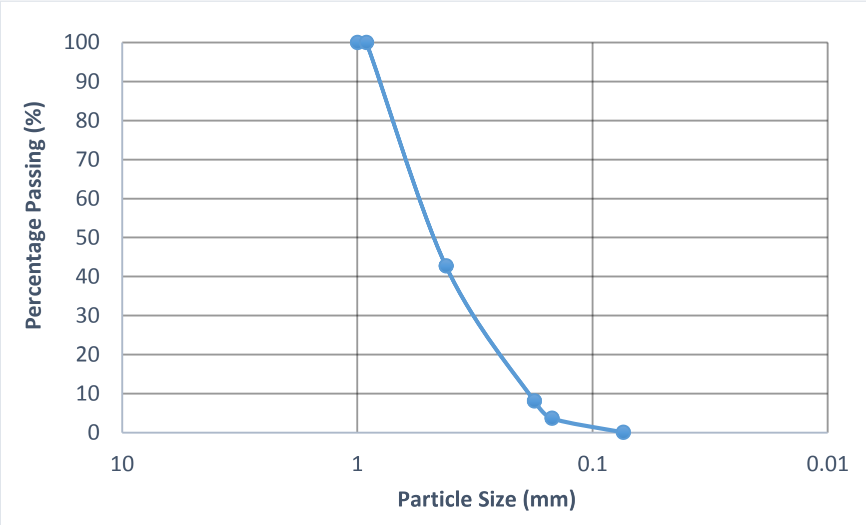

Figure 3.9 The sand's grain size distribution

3.9. Hand compactor

In this study,a hand compactor was used to determine the relative density of sand. The important thing about this machine was that it was compacted in this test with a steel tamper with dimensions (15cm x 15cm). The bottom of the steel plate has a plastic base with the same dimension of the steel plate that was contacted to the bottom of the steel base that is used to avoid crushing the sand practices, shown in Figure 3.10.

Figure 3.10 Hand compactor

3.10. Determination of relative densities of this experimental

Determination of relative densities was conducted in the laboratory by a series of trial tests according to ASTM D4253 – 16 [45], which determine the model tank's relative densities required to experiment. A wooden box (42 x 27.8 x 11.2) cm is used in the experiments. The sand was taken in the oven for twenty-four hours; then the dried sand was filled into a wooden box, several trials and error for conducting to determine four relative densities D_r =10%, Dr =40%, Dr =65%, Dr =90%. The procedure of determination relative densities have been described below:

1- A relative density of 10% of sand was normally pouring into the wooden box at the height of 15 cm by using the plastic hose.
2- A relative density of 40% was obtained by pouring sand into the wooden box from 10 cm and compacted by a hammer for one moment at each point (15×15cm).
3- A relative density of 65% was obtained by pouring sand into the wooden box from 10 cm and compacted by a hammer for two moments at each point (15×15cm).
4- A relative density of 90% was obtained by pouring sand into the wooden box from 10 cm and compacted by a hammer for eight moments at each point (15×15cm).

After conducting each trial of testing, each sample's relative density determines moisture content and dry unit weight. Table 3.5 indicates dry unit weight for each relative density. Shows the Figure 3.11 calibration of relative density in the laboratory.

Table 3.5 Dry unit weight and void ratio

Relative density %	Dry unit weight	Void ratio
10	14.6	0.86
40	15.5	0.75
65	16.3	0.66
90	17.3	0.57

 

Figure 3.11 Calibration of the relative density of sand.

3.11. Static Pile Load Tests

The static pile load test provides the most detailed indicator of the in-place pile capacity. It is carried out using a method of reaction. The research technique involves adding one hydraulic jack, an axial load, to the test pile's top. In the case of a compression static load test, the reaction force is transmitted through single piles that enter. In the case of a static load test, the data is compressed. Different types of instruments are set up on the test piles and the lever piles in order to achieve precise measurement of the pile displacement.

The static pile load testing reaches the ASTM D1143 [46] requirements, Method A: Easy Testing, each compression load test needs approximately 4 to 8 hours to perform for the static compressive load testing.

3.12. Procedure determination bearing capacity of open-ended piles

In this experiment, to determine the bearing capacity and skin friction for open-ended piles to describe the details of conducting the test and sketching all steps of the tests. This study has two open-ended piles, but the plugging dimension has different that the bearing capacity's procedure determination has the same procedure. The procedure of the experiment is the following steps:

1- Before starting the load test, the model tank must be cleaned and closed the tank's gate to avoid getting out of the sand particles on the tank's side.

2- The model of the tank is filled sand the height of 90cm, but each relative density has a different procedure for filling the model tank:

a) For relative density, 10%, the depth of the model tank dividing 9 nine layers each 10cm layers pouring by flexible plastic hose the height 15cm above the surface layers, but in this relative density don't need compaction shown the Figure 3.12 shows sand layer in relative density 10%.

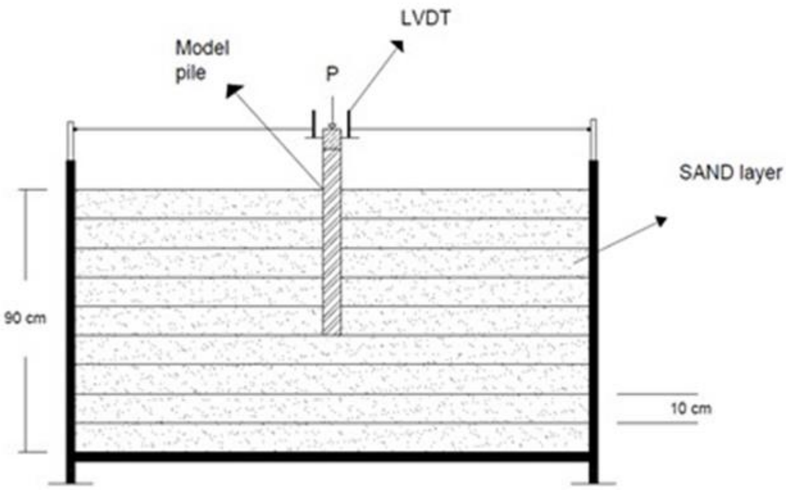

Figure 3.12 Bearing capacity determination of pile at D_r= 10%

b) Relative density 40%, the depth of the model tank is dividing 9 layers. Each layer is 10cm height. Pouring by flexible hose from the height 10 cm above surface layer, it can be seen in the Figure 3.13 shows sand layer in relative density 40%, each layer compacted each by the hand compactor machine for eight seconds.

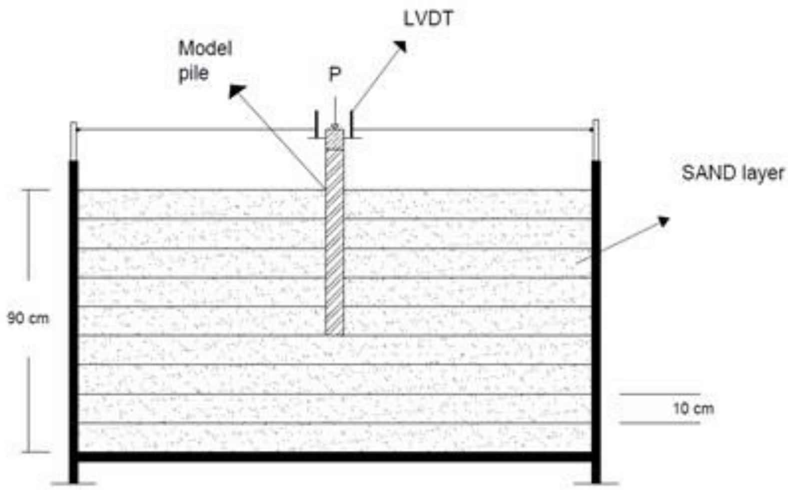

Figure 3.13 Bearing capacity determination of pile at D_r = 40%

c) Relative density 65%, the depth of the model tank is dividing 9 layers. Each layer is 10cm in height. Pouring by flexible hose from the height 10 cm above surface layer, it can be seen in Figure 3.14 shows sand layer in relative density 65%, each layer compacted each by the hand compactor machine for two seconds.

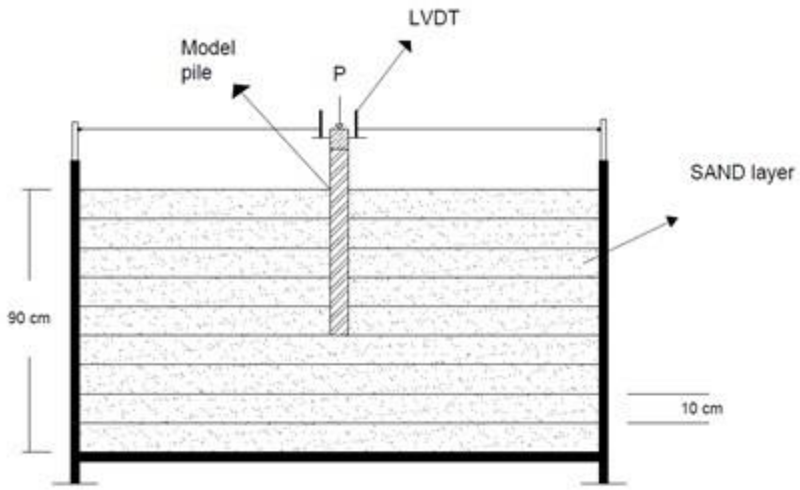

Figure 3.14 Bearing capacity determination of pile at Dr = 65%

d) Relative density 90%, the depth of the model tank is dividing 18 eighteen layers. Each layer is 5cm in height. Pouring by flexible hose from the height 10 cm above surface layer, it can be seen in Figure 3.15 shows sand layer in relative density 90%, each layer compacted each by the hand compactor machine for eight seconds.

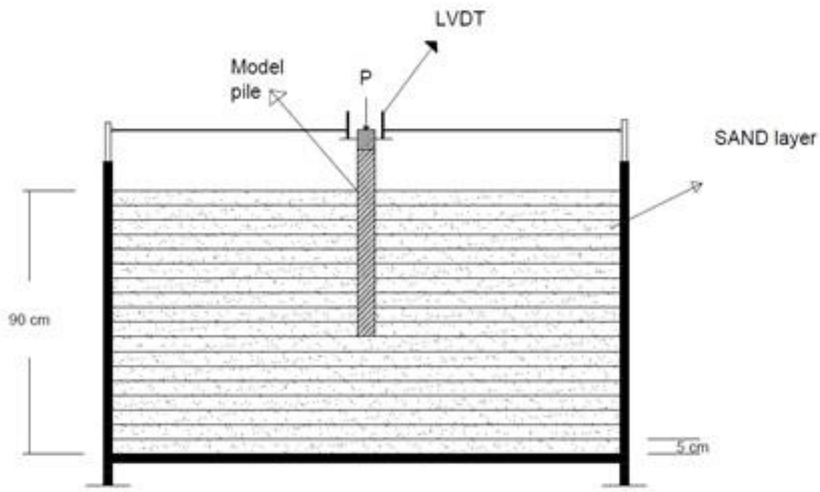

Figure 3.15 Bearing capacity determination of pile at $D_r = 90\%$

3- When the model of the tank filled 40cm the installing the pile attached the load cell, capacity 5 tons, by using epoxy, the load cell and pile connecting the hydraulic jack. After that, the piles installed and moved down until the base of the pile touched on the surface to the soil which can be seen in Figure 3.16 shows the sand layer.

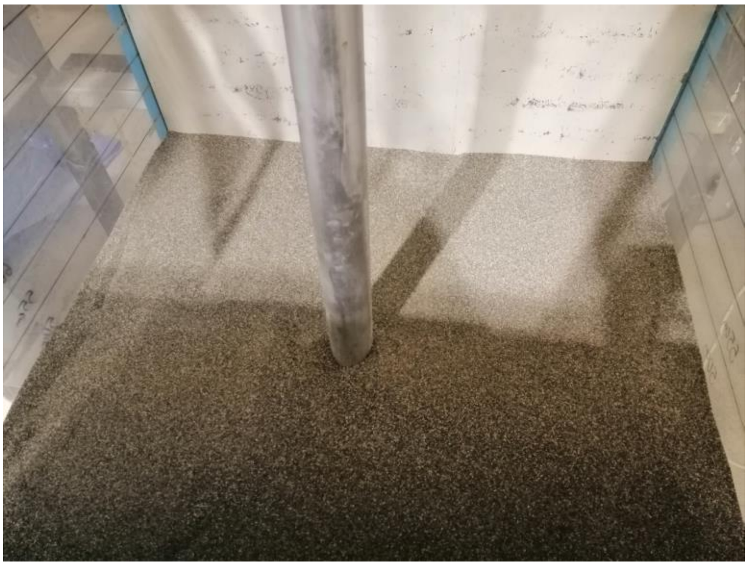

Figure 3.16 Pile installed in the model tank

4- After the pile was installed, the model of tank-filled sand above 90 cm height. The two LVDTs (15 cm length) was settled left, and right side of the pile head can be seen in Figure 3.17

Figure 3.17 Two LVDTs installed in the model of experiment

5- Turn on the computer controlling system that was used to operate the hydraulic jack; The axial load was applied to the pile by using a computer controlling system. The loading machine used in this study for loading control. The vertical displacement rate is approximately (1 mm/min)

6- Computer programming uses recorded data of load and displacement shown the Figure 3.18 indicate all part of the computer. The data was measured by Keli S-type 5 ton capacity load cell and two LVDTs that both data can obtain bearing capacity of the pile.

Figure 3.18 Computer machine using in the test

3.13. Direct shear test for the sand

The soil's main engineering characteristic is shear strength, which, under structural loads, determines the strength of the soil mass. Various geotechnical constructions are designed, It is critical to accurately determine soil shear strength characteristics (internal friction and cohesion angles). These parameters may be measured in the lab or in the field. The direct shear and triaxle compression tests are the most commonly used in laboratories to determine shear resistance angle and cohesion values. Special care must be taken to create a loading situation in the and replicate it in the laboratory [47].

In designs made by geotechnical designers, the skin friction angle between soil and pile materials is a major aspect. Frictional forces create civil engineering structures between structures and the soil. Retaining walls, sheet piles, diaphragm walls, and piles are examples. As is well established, the effect on loose, sandy soils of the resistance to pile tips is underestimated and the carrying capacities are completely proportional to the friction of the skin. Therefore, the skin friction angle in geotechnical design is known to be important [48].

In the direct shear test, a sand sample is put in the shear box. The standard dimension of the sample (6 x 6 x 2) cm, for determination of the internal friction angle (φ) of sand and the skin friction angle (δ) between sand and steel piles at each relative density.

3.13.1. Determination of internal friction angles (ϕ) of sand

In this study, each relative density (D_r=10%, D_r=40%, Dr=65%, D_r=90%) samples were prepared in a direct shear box to determine the internal friction angle. In three direct shear tests, three direct shear experiments were carried out. Various normal stresses (54.5, 109, and 163.5 kPa) according to ASTM D5321/D5321M-14 [49]. Table 3.6 shows the findings of the testing. The internal friction angle of sand increases as the relative density of the sand increases, as seen in Figure 3.19.

Table 3.6 The sand's internal friction angle versus the relative density of the sand [50].

The relative density of the sand (Dr = %)	Internal friction angle of the sand (ϕ)
10	41.0°
40	44.3°
65	48.7°
90	52.4°

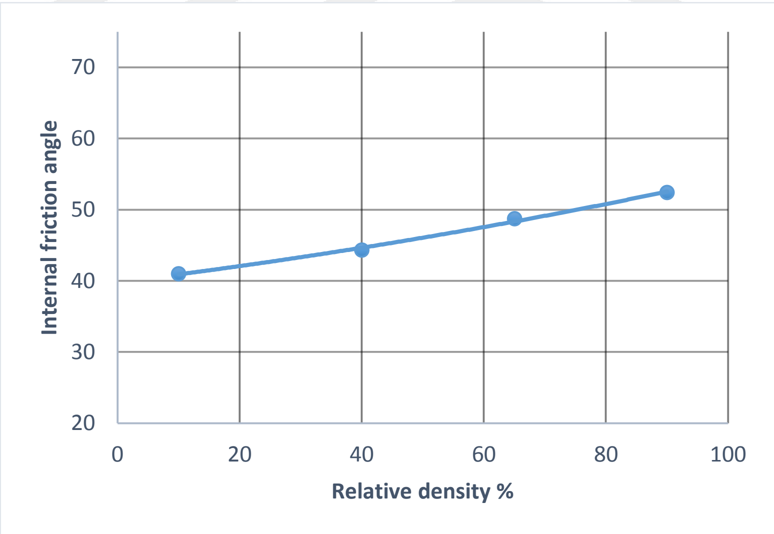

Figure 3.19 The internal friction angle of the sand corresponding to relative densities

3.13.2. Determination skin friction angle (δ) between sand and steel piles

After determining the internal friction angle, the interface skin friction angle was determined for each relative density. The interface friction angle between sandy soil and piles of steel was measured with different relative densities for three normal stresses (54.5, 109, and 163.5 KPa) at a constant rate of 0.5 mm/min depending on ASTM D5321/D5321M-14 [49]. Table 3.7 displays the results. As can be seen in Figure 3.20, the skin friction angle rises with increasing relative density up to Dr = 60%, but then starts to decrease at Dr = 90%.

Table 3.7 The skin friction angle between sand and steel pile [50].

Relative density of the sand (Dr = %)	Skin friction angle (δ) between sand and steel piles
10	18.04°
40	19.28°
65	20.7°
90	18.8°

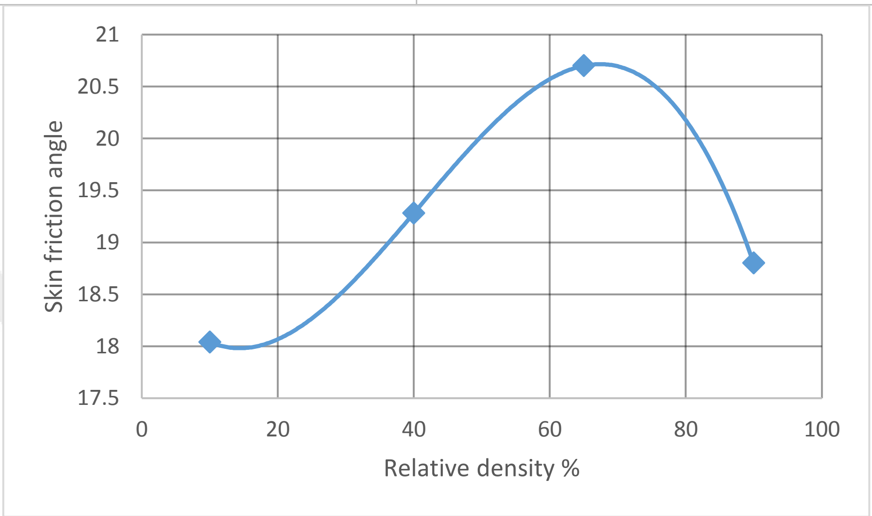

Figure 3.20 Skin friction angle between sand and piles steel corresponding relative densities.

4. RESULTS AND DISCUSSION

4.1. General

The details and experimental results of model piles are presented in this chapter and compared to the finite element results.

4.1.1. Experimental results

In the laboratory, the load-settlement curves are determined by using a pile-load test, representing the relationship between load and settlement. The load-settlement curves for both pile A and pile B with different relative densities (10%, 40%, 65%, 90%) are shown in Figure 4.1 to Figure 4. 4.

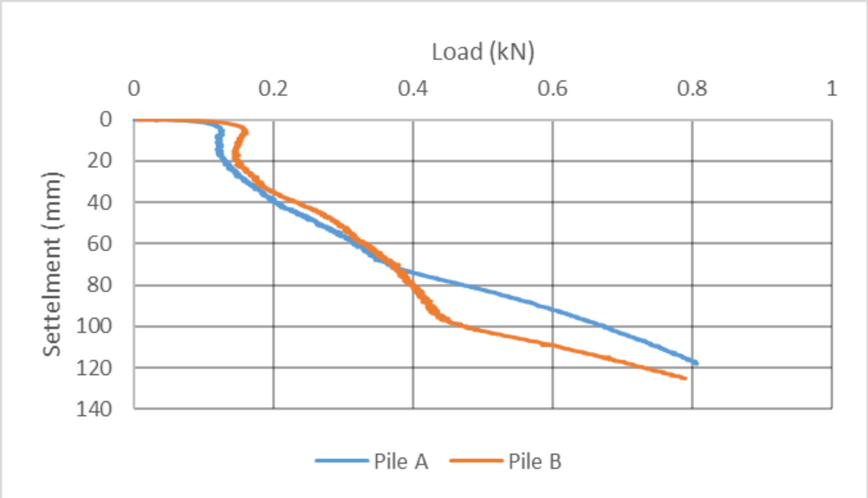

Figure 4.1 Load-settlement curves for both piles in Dr = 10%

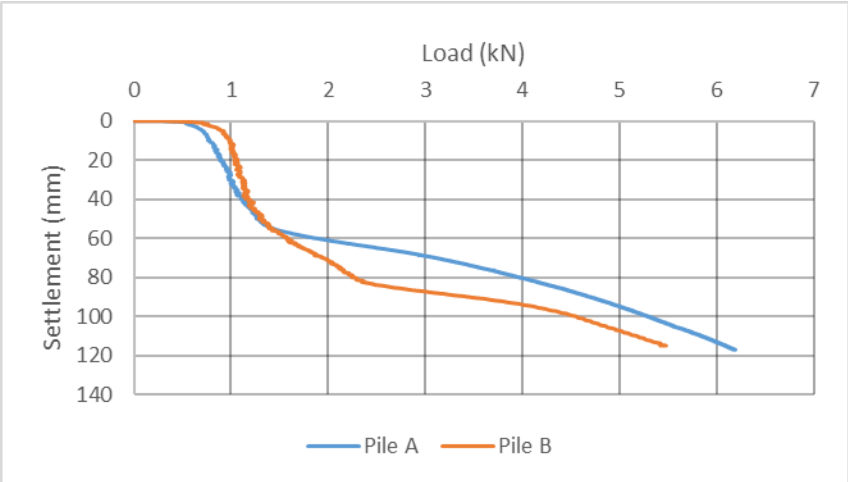

Figure 4.2 1 Load-setelment curves for both piles in Dr = 40%

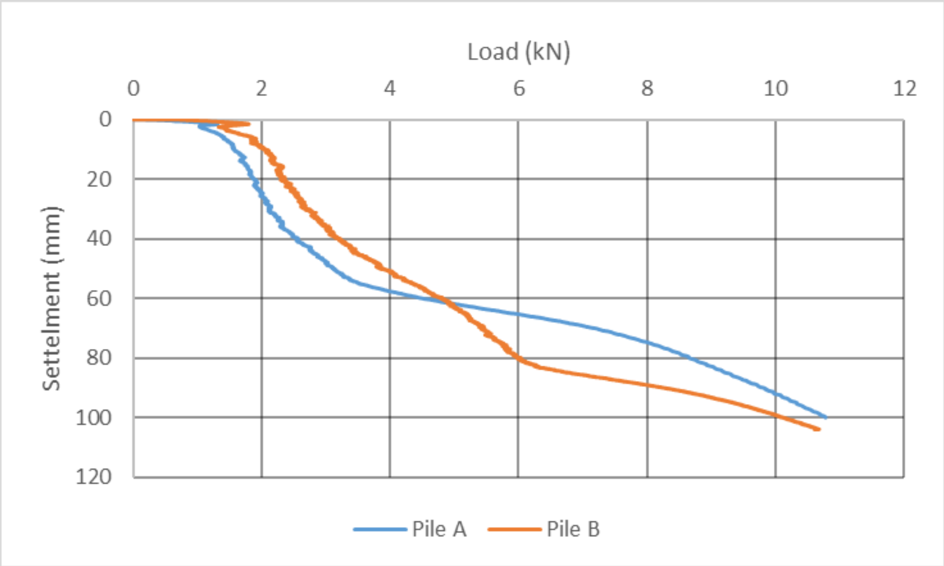

Figure 4.3 Load-settlement curves for both piles in Dr = 65%

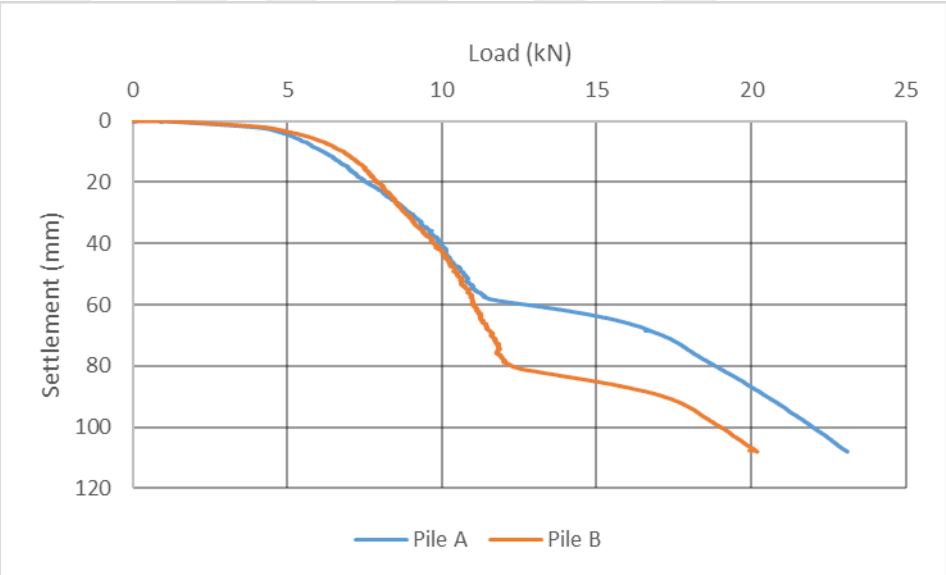

Figure 4.4 Load-settlement curves for both piles in Dr = 90%

The ultimate bearing capacity determined in pile load tests can be seen in Table 4.1 and Table 4.2. The ultimate bearing capacity of both piles increases as the relative density increases. The settlement, which corresponds to the ultimate bearing capacity, decreases as the relative density increases. The results of the two model piles showed that pile B has a higher capacity than pile A when the relative density increases. Figure 4.5 shows the ultimate bearing capacity of two piles with different relative densities of sand. Figure 4.6 shows the settlement of two piles with different relative densities of sand.

Table 4.1 The ultimate bearing capacity of pile A

Relative density %	Load (kN)	Settlement (mm)
10	0.48	80.98
40	4.06	80.35
65	7.2	70
90	16.1	66.37

Table 4.2 The ultimate bearing capacity of pile B

Relative density %	Load (kN)	Settlement (mm)
10	0.568	106.93
40	4.2	95.87
65	8	89.08
90	16.7	88.6

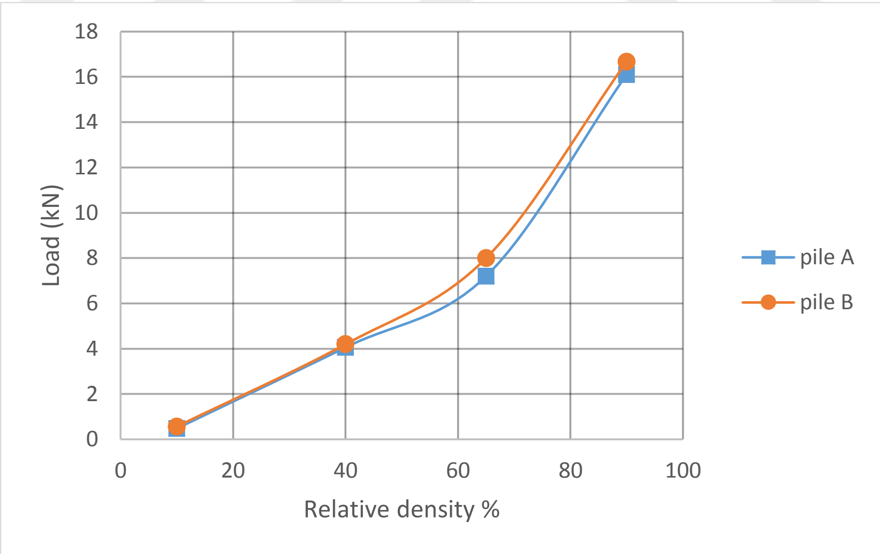

Figure 4.5 Variation between load and relative densities for both piles

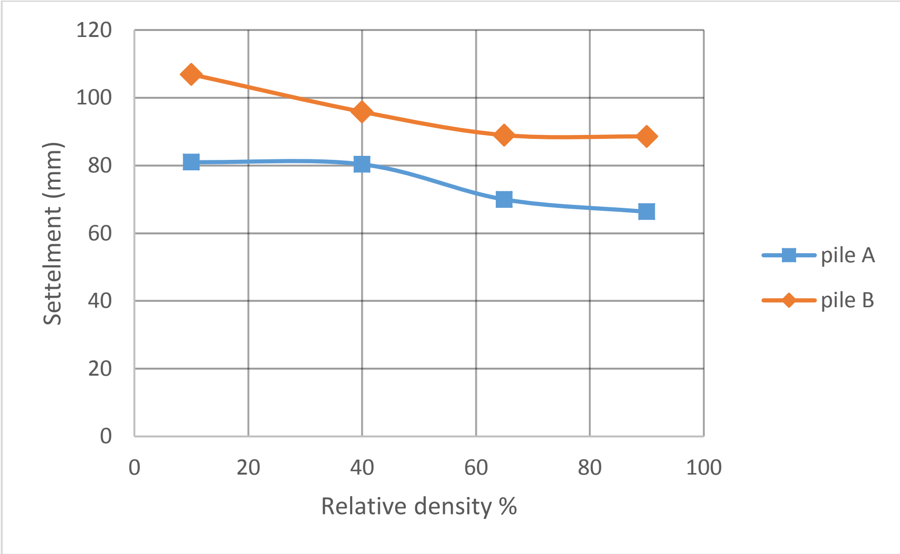

Figure 4.6 Variation between settlement and relative densities for both pile

4.2. Finite element analysis

Three-dimensional numerical simulation analysis was conducted to compare the results of the model tests and evaluate the stress distributions generated by the sand pile. The finite element was carried out using the Plaxis 3D V20 package program, which corresponds to the finite element approach. The loading conditions, the test tank, and the Plaxis computer software were used to account for the model pile and material characteristics. Figure 4.7. The sand characteristics were simulated using the Mohr-Coulomb model.

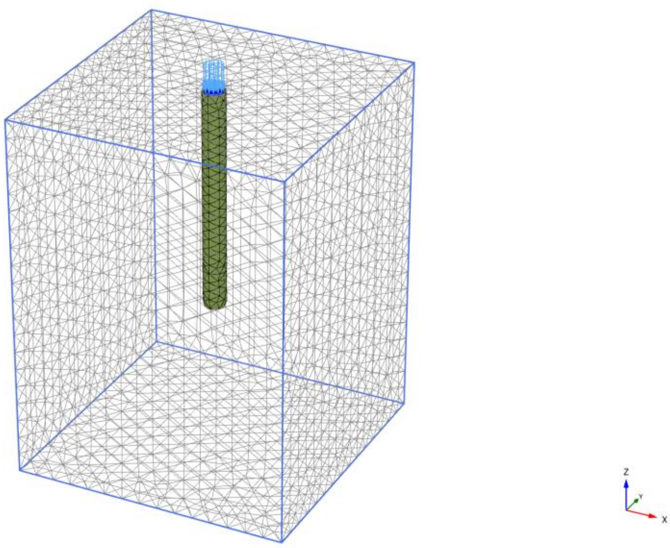

Figure 4.7 Modelling tank

4.2.1. Plaxis 3D software

Plaxis software has been used to evaluate and solve geotechnical issues using the finite element technique, which depends on computer modeling calculation accuracy. Given the results of the numerical analysis that addressed the geotechnical and model tests in the laboratory, performance estimates are anticipated. The software for modeling the material testing comes in two flavors: 3D and 2D. We utilized 3D in this research.

4.2.2. Parameters of material used in Plaxis 3D

The sand was simulated using the Mohr-Coulomb failure criteria, and the dry unit weight of the sand corresponding to relative density was entered into the Plaxis 3D. Both piles were modeled using linear elastic and non-porous materials, and their unit weights were entered into the Plaxis 3D software. The specifications of the sand piles used in Plaxis 3D are shown in Table 4.3. The specifications of both pile materials used in Plaxis 3D are shown in Table 4.4

Table 4.3 The sand parameters for both piles entered into Plaxis 3D

Relative density %	Dry Unit weight (kN/m^3)	Modulus of Elasticity of the Sand (E) (kN/m^2)	Poisson's ratio	Internal friction angle of the sand (φ)°	Dialatancy angle of the sand(ψ)°	R_{int}	Cohesion (kN/m^2)
10	14.6	3500	0.3	41	11	0.7	0.001
40	15.5	48250	0.3	44.3	14.3	0.7	0.1
65	16.3	67000	0.3	48.7	18.7	0.7	0.3
90	17.3	89900	0.3	52.4	22.4	0.7	0.5

Table 4.4 The model piles parameters entered into Plaxis 3D

Model pile	Dry Unit Weight (kN/m^3)	Modulus of Elasticity of the Sand (E) (kN/m^2)	Poisson's ratio
Steel pile	78.5	2×10^8	0.3

4.3. Results of Plaxis 3D

After the total bearing capacity was determined from the experimental curves for both piles, the sand and pile models were prepared for Plaxis 3D and, using parameters mentioned in the table above, the same value of total bearing capacity of both piles was determined in the experimental load-settlement curves used in Plaxis 3D. Figure 4.8 to Figure 4.15 show the load-settlement curves for both piles (pile A and pile B) in Plaxis 3D at various relative densities.

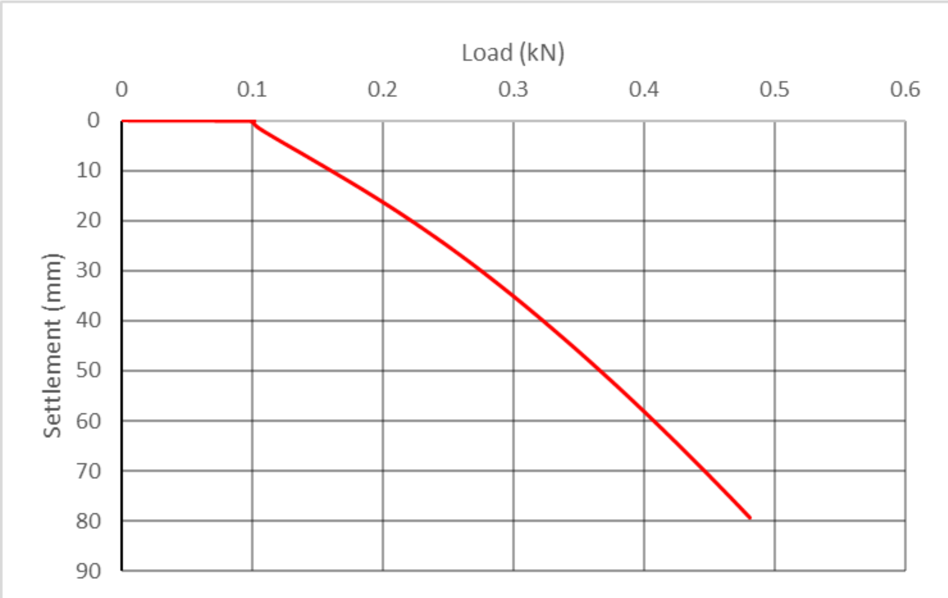

Figure 4.8 Load-settlement curves in Plaxis 3D for pile A in Dr = 10%

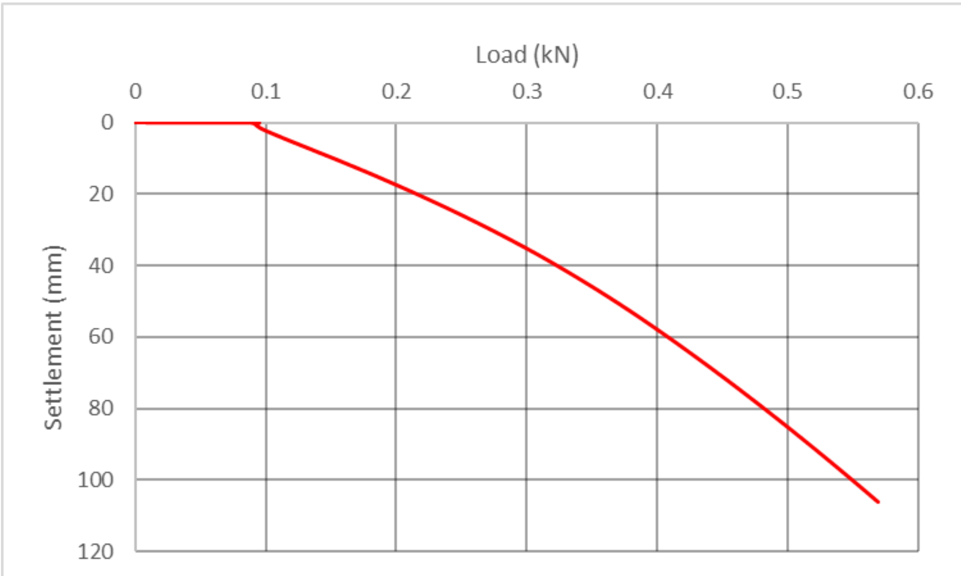

Figure 4.9 Load-settlement curves in Plaxis 3D for pile B in Dr = 10%

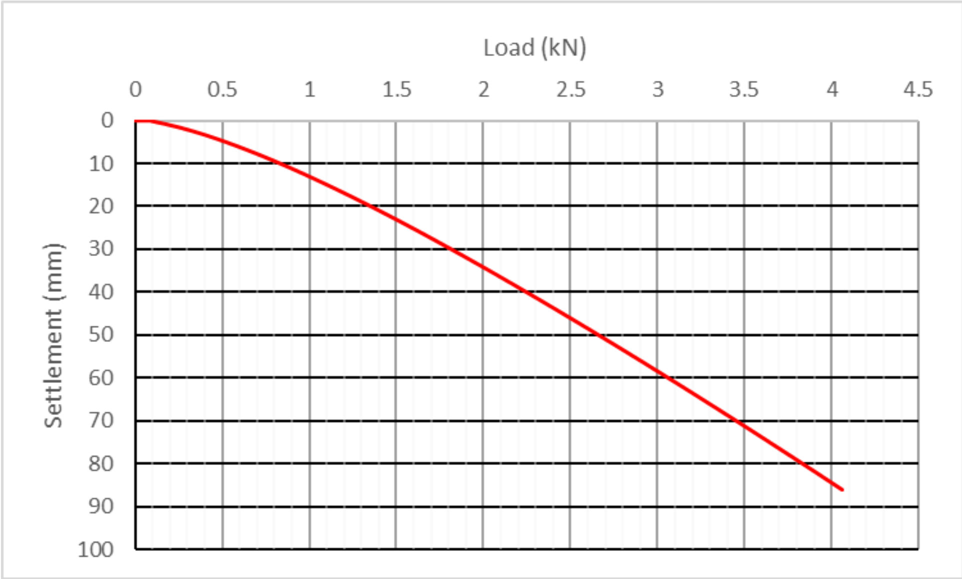

Figure 4.10 Load-settlement curves in Plaxis 3D for pile A in Dr = 40%

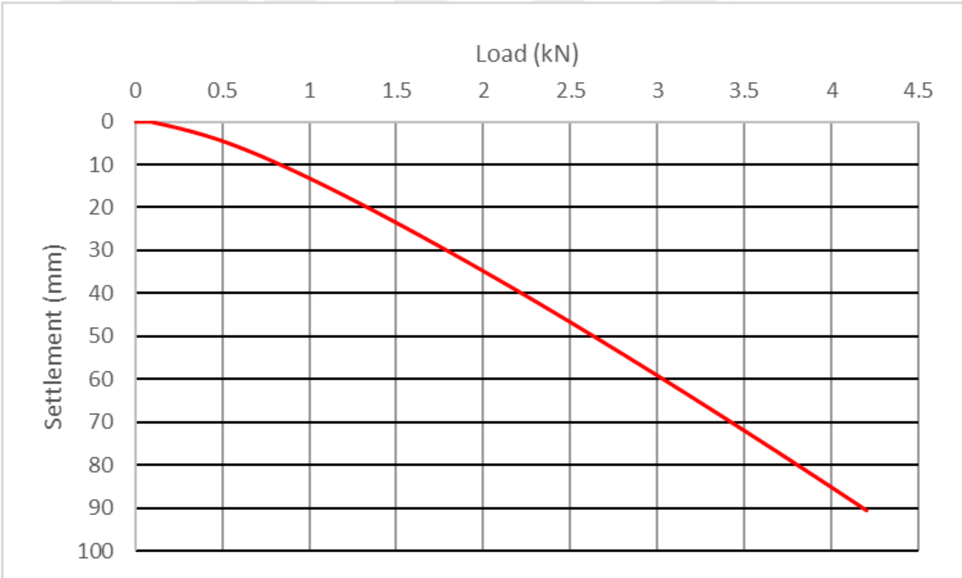

Figure 4.11 Load-settlement curves in Plaxis 3D for pile B in Dr = 40%

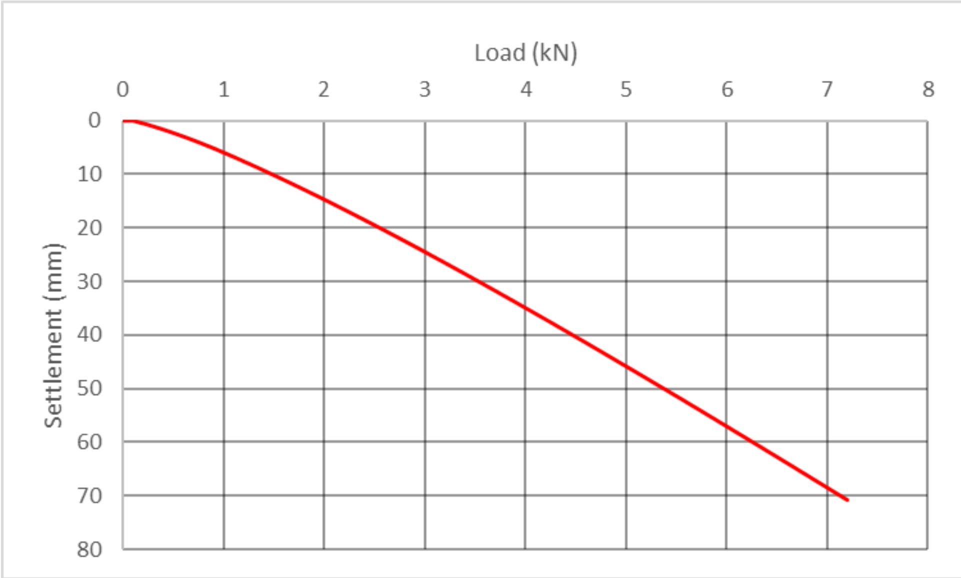

Figure 4.12 Load-settlement curves in Plaxis 3D for pile A in Dr = 65%

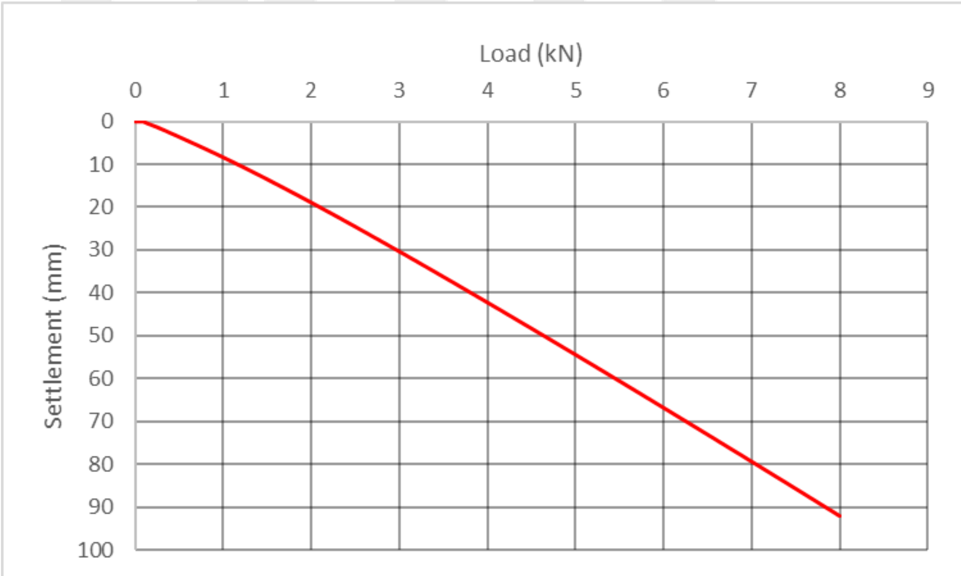

Figure 4.13 Load-settlement curves in Plaxis 3D for pile B in Dr = 65%

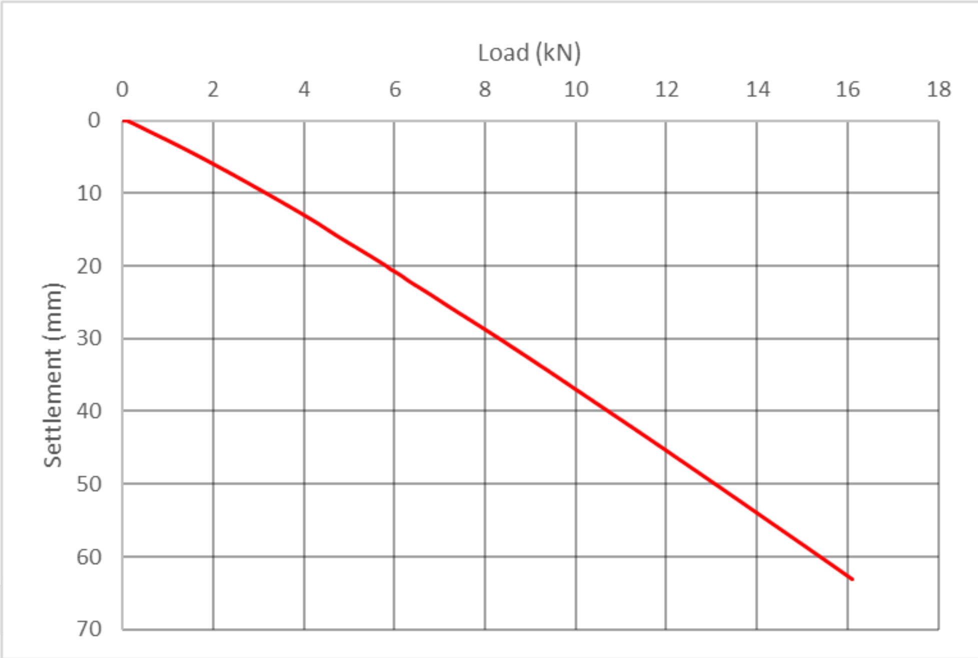

Figure 4.14 Load-settlement curves in Plaxis 3D for pile A in Dr = 90%

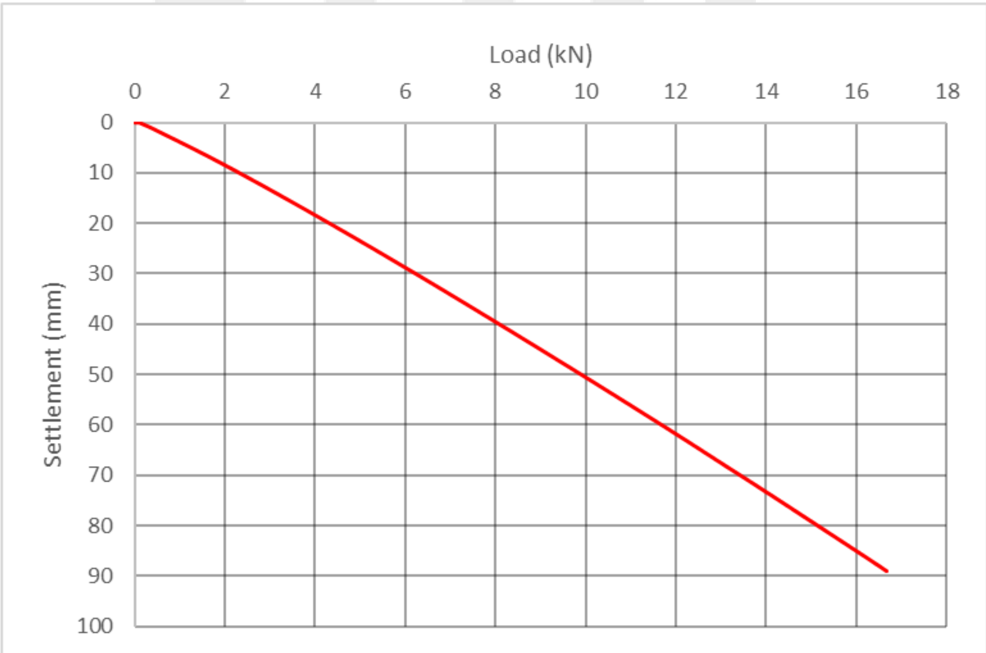

Figure 4.15 Load-settlement curves in Plaxis 3D for pile B in Dr = 90%

According to the results shown in Tables 4.5 and 4.6, the Plaxis 3D finite element software agrees well with the experimental results. In Figure4.16, the relation between pile A's experimental and Plaxis 3D settlement results with relative densities can be seen. Figure4.17: The relation between pile B's experimental and Plaxis 3D settlement results with relative densities can be seen.

Table 4.5 The results of the comparison between experimental and Plaxis 3D were obtained. For pile A

Relative density %	Load (kN)	Experimental Settlement (mm)	Plaxis 3D Settlement (mm)
10	0.4825	80.988	79.09
40	4.06	80.35	86.1
65	7.2	70	70.84
90	16.1	66.37	63.02

Table 4.6 The results of the comparison between experimental and Plaxis 3D were obtained. for pileB

Relative density %	Load (KN)	Experimental Settlement (mm)	Plaxis 3D Settlement (mm)
10	0.568	106.935	106.18
40	4.2	95.874	90.45
65	8	89	92.14
90	16.67	88.6	88.98

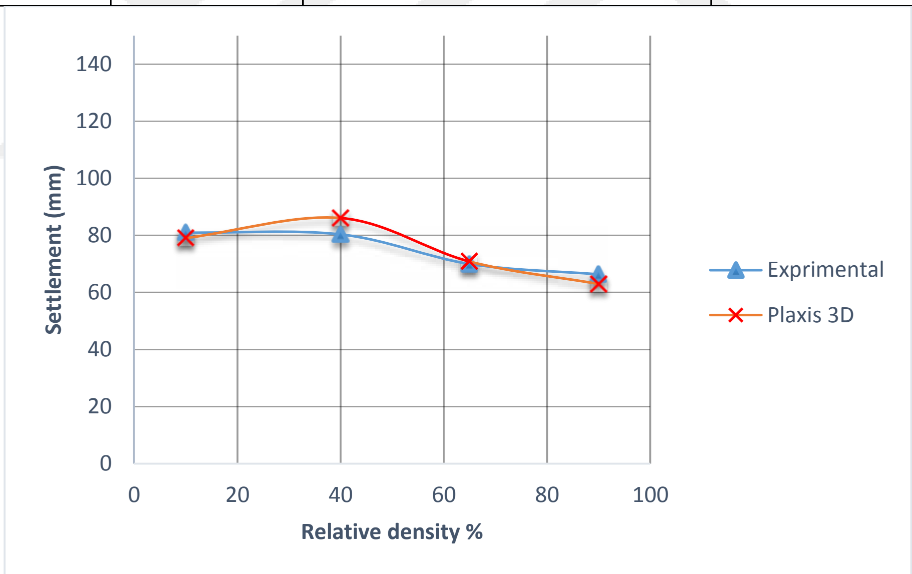

Figure 4.16 Comparison of experimental and Paxis 3D results for pile A

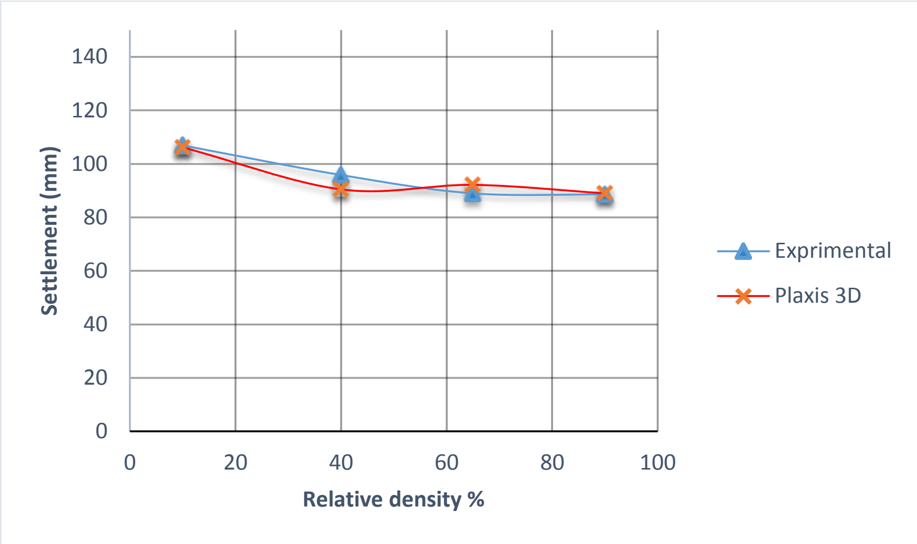

Figure 4.17 Comparison of experimental and Paxis 3D results for pile B

5. CONCLUSIONS

In this study, it investigated the ultimate bearing capacity and load-settlement behavior of two model open-ended piles at different relative densities (Dr=10%, Dr=40%, Dr=65%, Dr=90%) of model sand that was conducted in the pile-load test. Plaxis 3D finite element software was used to build a numerical model of the experimental system, and simulations for specific loading tests were performed. The results of the tests led to the following conclusions:

1- According to the pile load test results, the ultimate bearing capacity of both piles increases with increasing relative density, but the settlement of the ultimate bearing capacity decrease with increasing relative density.
2- From the comparison between pile A and pile B results, it was discovered that pile B's ultimate bearing capacity and settlement were greater than those of pile A.
3- The total bearing capacity load-settlement curves show that the total bearing capacity mobilized at the settlement is about (10-20) percent of the pile model diameter.
4- From finite element analysis, it was discovered that the finite element results and experimental results are in good agreement because they are not far from each other and are very close.

There is a recommendation that I want to use a fiber-reinforced polymer (FRP) pile instead of an open-ended steel pile. The pile has the same diaphragm, but it is determined bearing capacity compared with an open-ended steel pile.

REFERENCES

[1] Abeb, *Pile Foundation Design-A Student Guide*, in *School of Built Environment*2005: Napier University, Edinburgh.

[2] Paik, K. and Salgado, R. (2003). Determination of bearing capacity of open-ended piles in sand, *Journal of Geotechnical and Geoenvironmental Engineering*, C Vol. 129 (1), pp: 46-57.

[3] Das, B.M., (2019). *Principles of Foundation Engineering*,

[4] Prakash, S. and Sharma, H.D., (1990). *Pile foundations in engineering practice*, John Wiley & Sons,

[5] Skempton, A. (1959). The Boat Store, Sheerness (1858-60) and its place in structural history, *Transactions of the Newcomen Society*, C Vol. 32 (1), pp: 57-78.

[6] Burland, J. (1973). Shaft friction of piles in clay--a simple fundamental approach, *Publication of: Ground Engineering/UK/*, C Vol. 6 (3), pp.

[7] Focht, J.A. and Vijayvergiya, V. (1972). A new way to predict capacity of piles in clay. in *Offshore Technology Conference*. Offshore Technology Conference.

[8] C.Venkatramaiah, (2006). *Geotechnical Engineering*, S.V University college of Engineering Tirupati,India

[9] Sharma, S.P.a.H.D., (1990). *Pile Foundations in Engineering Practice*,

[10] Hollaway, L. (2010). A review of the present and future utilisation of FRP composites in the civil infrastructure with reference to their important in-service properties, *Construction and building materials*, C Vol. 24 (12), pp: 2419-2445.

[11] Guades, E.J., Aravinthan, T., Islam, M., and Manalo, A.C. (2012). Stiffness of FRP pultruded tubes under repeated axial impacts. in *Proceedings of the 3rd Asia-Pacific Conference on FRP in Structures (APFIS 2012)*. International Institute for FRP in Construction (IIFC).

[12] Iskander, M.G. and Hassan, M. (1998). State of the practice review in FRP composite piling, *Journal of Composites for Construction*, C Vol. 2 (3), pp: 116-120.

[13] Pando, M.A., Filz, G.M., Dove, J.E., and Hoppe, E.J., *Interface shear tests on FRP composite piles*, in *Deep Foundations 2002: An International Perspective on Theory, Design, Construction, and Performance*2002. p. 1486-1500.

[14] Guades, E., Aravinthan, T., Islam, M., and Manalo, A. (2012). A review on the driving performance of FRP composite piles, *Composite Structures*, C Vol. 94 (6), pp: 1932-1942.

[15] Das, B.M., (2004). *Pile foundations, Principles of Foundation Engineering.*, California, USA: Brooks/Cole-Thomson Learning

[16] Murthy, V.N.S., (2002). *Principles and Practices of soil mechanic and foundation Engineering*,

[17] Kishida, H. (1977). Behavior of sand plugs in open-end steel pipe piles. in *Proc. of the 9th Int. Conf. on SMFE*.

[18] Klos, J. and Tejchman, A. (1977). Analysis of behavior of tubular piles in subsoil. in *Proc., 9th Int. Conf. on Soil Mechanics and Foundation Engineering*.

[19] Woodward., M.T.a.J., (1994). *Foundation design and construction*,

[20] Al-Soudani, W.H. and Albusoda, B.S. (2021). An Experimental Study on Bearing Capacity of Steel Open Ended Pipe Pile with Exterior Wings Under Compression Load, *Geotechnical and Geological Engineering*, C Vol. 39 (2), pp: 1299-1318.

[21] Ulitskii, V. (1995). History of pile foundation engineering, *Soil Mechanics and Foundation Engineering*, C Vol. 32 (3), pp: 110-114.

[22] Szechy, C. (1961). The effect of vibration and driving upon the voids in granular soil surrounding a pile. in *Proceedings of the 5th international conference on Soil Mechanics and Foundation Engineering*.

[23] Paik, K.H. and Lee, S.R. (1993). Behavior of soil plugs in open-ended model piles driven into sands, *Marine Georesources & Geotechnology*, C Vol. 11 (4), pp: 353-373.
[24] Klos, J. and Tejchman, A. (1981). Bearing capacity calculation for pipe piles. in *Proceedings of the 10th International Conference on Soil Mechanics and Foundation Engineering, Stockholm, Sweden*.
[25] Al-Mhaidib, A.I. (1999). Bearing capacity of a model pile in sand under different loading rates. in *The Ninth International Offshore and Polar Engineering Conference*. International Society of Offshore and Polar Engineers.
[26] Lehane, B., Schneider, J., and Xu, X. (2005). The UWA-05 method for prediction of axial capacity of driven piles in sand, *Frontiers in offshore geotechnics: ISFOG*, C Vol. 683-689.
[27] Kikuchi, Y., Mizutani, T., Morikawa, Y., and Sato, T. (2010). Plugging mechanism of open-ended piles, *Soil-foundation-structure interaction. London: Taylor & Francis Group*, C Vol. 27-32.
[28] Fattah, M.Y. and Al-Soudani, W.H. (2016). Bearing capacity of open-ended pipe piles with restricted soil plug, *Ships and Offshore Structures*, C Vol. 11 (5), pp: 501-516.
[29] Liu, J., Guo, Z., and Han, B. (2019). Load transfer of offshore open-ended pipe piles considering the effect of soil plugging, *Journal of Marine Science and Engineering*, C Vol. 7 (9), pp: 313.
[30] Guo, Y., Dong, S., Li, J., and Yu, X.B. (2020). Numerical and Experimental Study on Soil Plug Resistance of Open-Ended Pipe Pile with a Restriction Plate, *Advances in Civil Engineering*, C Vol. 2020.
[31] Randolph, M. (1987). Modelling of the soil plug response during pile driving. in *Southeast Asian geotechnical conference. 9*.
[32] Aksoy, H., Inal, E., and Gor, M. (2016). Skin friction between soil and pile materials. in *Proceedings of the 12th International Congress on Advances in Civil Engineering, Istanbul, Turkey*.
[33] Paikowsky, S.G., Whitman, R.V., and Baligh, M.M. (1989). A new look at the phenomenon of offshore pile plugging, *Marine Georesources & Geotechnology*, C Vol. 8 (3), pp: 213-230.
[34] Paikowsky, S.G. and Whitman, R.V. (1990). The effects of plugging on pile performance and design, *Canadian Geotechnical Journal*, C Vol. 27 (4), pp: 429-440.
[35] Jeong, S., Ko, J., Won, J., and Lee, K. (2015). Bearing capacity analysis of open-ended piles considering the degree of soil plugging, *Soils and Foundations*, C Vol. 55 (5), pp: 1001-1014.
[36] Naghibi, F., Fenton, G.A., and Griffiths, D. (2014). Prediction of pile settlement in an elastic soil, *Computers and Geotechnics*, C Vol. 60 29-32.
[37] Kishanrao, W.M., Arun Prasad, A. (2016). Numerical Modeling Of Single Pile In A Two-Layered Soil, *International Journal of Mechanical and Production Engineering*, C Vol. 4 (6), pp.
[38] Han, F., Salgado, R., Prezzi, M., and Lim, J. (2017). Shaft and base resistance of non-displacement piles in sand, *Computers and Geotechnics*, C Vol. 83 184-197.
[39] Bolton, M.D., Gui, M.-W., Garnier, J., Corte, J.F., Bagge, G., Laue, J., and Renzi, R. (1999). Centrifuge cone penetration tests in sand, *Géotechnique*, C Vol. 49 (4), pp: 543-552.
[40] Taylan, Z. (2013). Experimental and numerical modeling studies for interpreting and estimating the δ behavior of single piles in unsaturated soils, *Graduate School of Science Engineering and Technology, Istanbul Technical University, Istanbul, Turkey*, C Vol.
[41] D422-63, A., (2007). *Standard Test Method for Particle-Size Analysis of Soils,American Test Methods Standards*, West Conshohocken,PA,
[42] D854-14, A., (2014). *Standard Test Methods for Specific Gravity of Soil Solids by Water Pycnometer, American Test Methods Standards,*, West Conshohocken, PA

[43] D854-83, A., (1989). *Standard test method for specific gravity of soils, Annual Book of Standards*, West Conshohoken
[44] Bairagi, H., Yadav, R., and Jain, R. (2014). Effect of jute fibres on engineering characteristics of black cotton soil, *ratio*, C Vol. 15 20.
[45] Standard, A., D4253-16. (2016). Standard Test Methods for Maximum Index Density and Unit
Weight of Soils Using a Vibratory Table, *ASTM International, West Conshohocken*, C Vol. (www.astm.org), pp.
[46] Zhang, L. (2004). Reliability verification using proof pile load tests, *Journal of Geotechnical and Geoenvironmental Engineering*, C Vol. 130 (11), pp: 1203-1213.
[47] Dirgėlienė, N., Skuodis, Š., and Grigusevičius, A. (2017). Experimental and numerical analysis of direct shear test, *Procedia Engineering*, C Vol. 172 218-225.
[48] Aksoy, H.S., Gor, M., and Inal, E. (2016). A new design chart for estimating friction angle between soil and pile materials, *Geomechanics and Engineering*, C Vol. 10 (3), pp: 315-324.
[49] D5321/D5321M-14, A., (2014). *Standard test method for determining the shear strength of soil-geosynthetic and geosynthetic-geosynthetic interfaces by direct shear*, ASTM International, West Conshohocken, PA, USA.
[50] Taher,N.R., (2019). *Firat University*. Ph.D. thesis, https://tez.yok.gov.tr/UlusalTezMerkezi/, Civil Engineering

Appendices

Appendix- 1: Experimental Time-Load and Time-settlement Curves of pile A

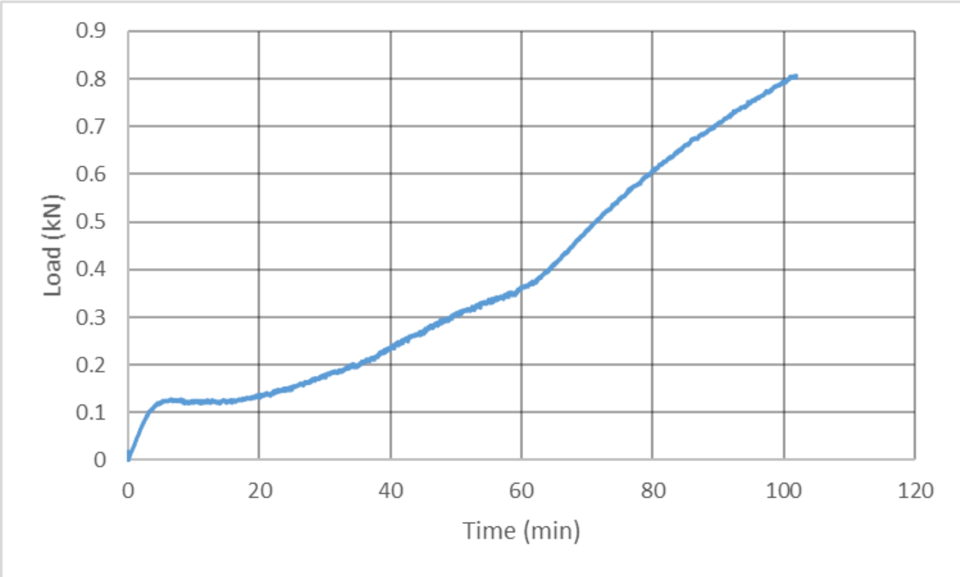

Figure A1.1. Time-Load curve for pile A in D_r=10%

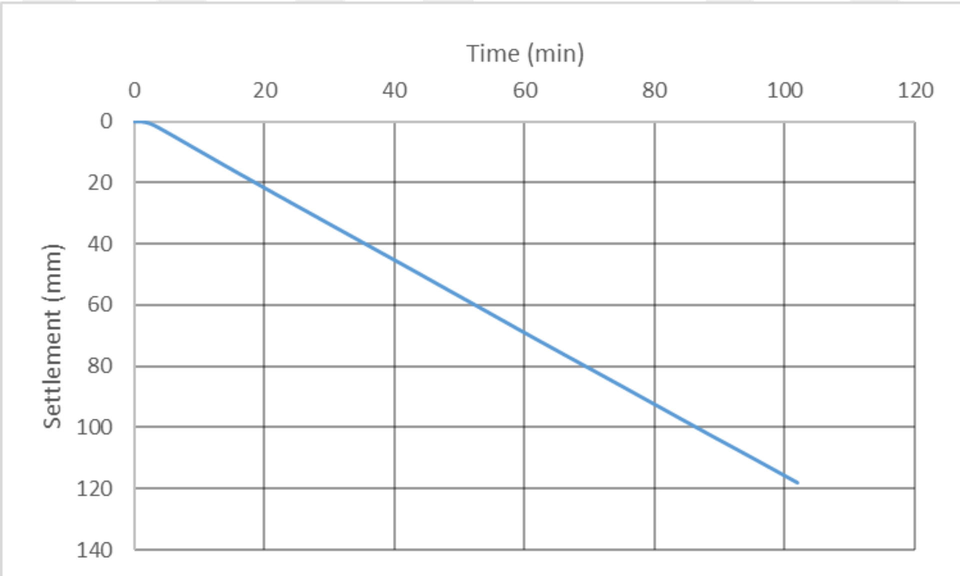

Figure A1.2. Time-Settlement curve for pile A in D_r=10%

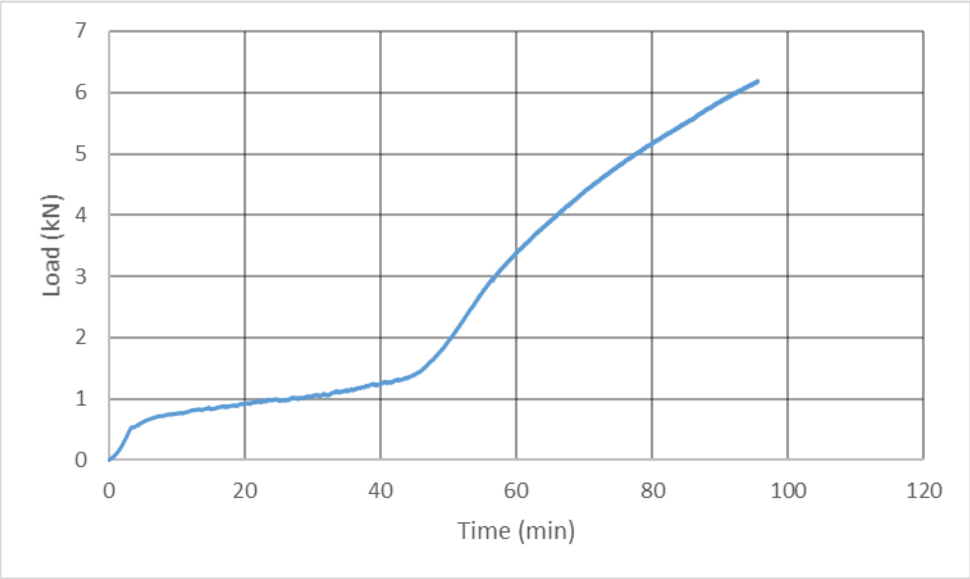

Figure A1.3. Time-Load curve for pile A in Dr=65%

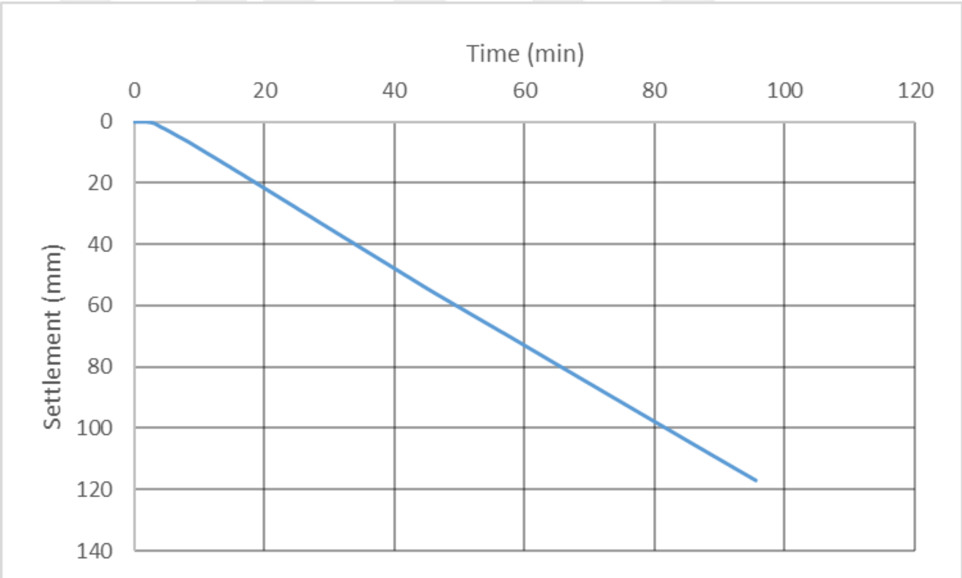

Figure A1.4. Time-Settlement curve for pile A in Dr=40%

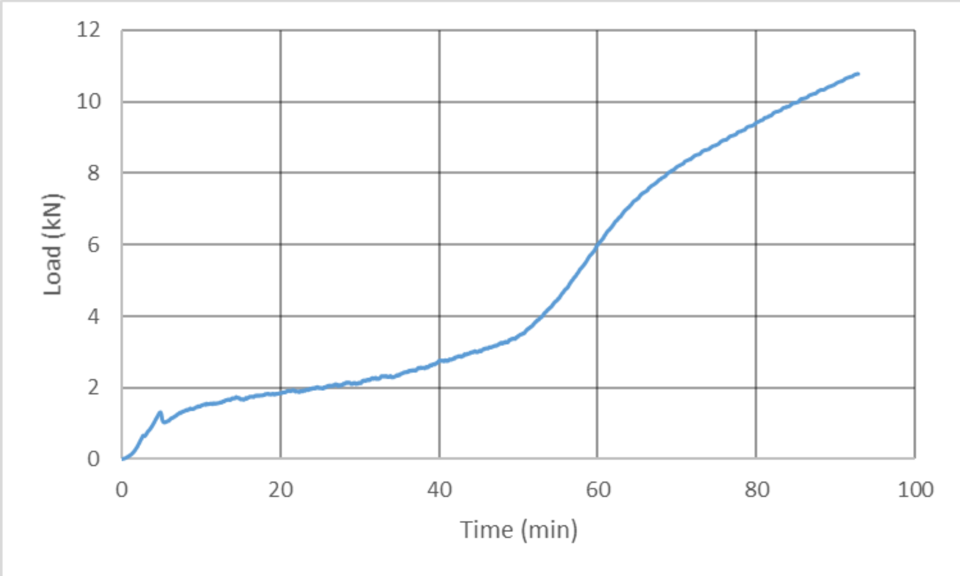

Figure A1.5. Time-Load curve for pile A in Dr=65%

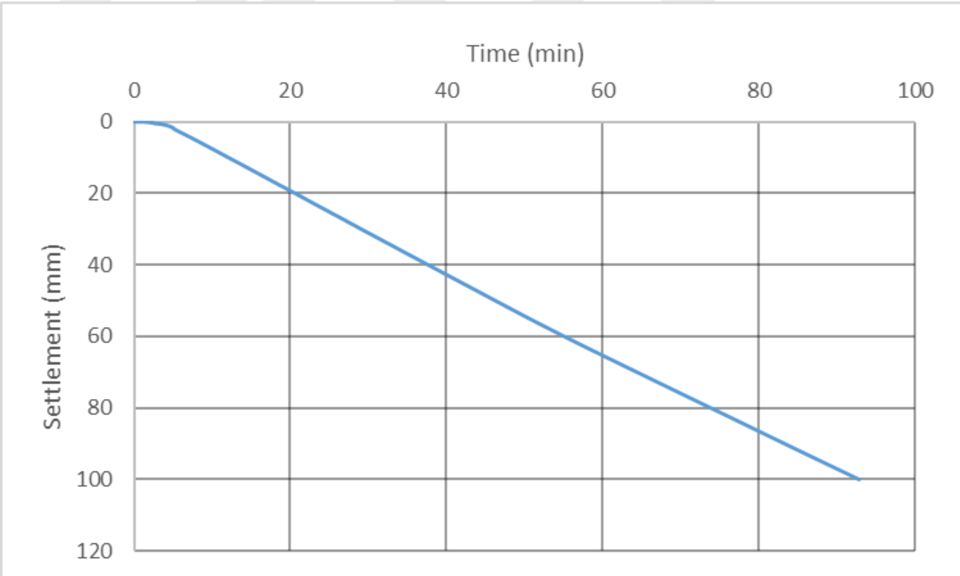

Figure A1.6. Time-Settlement curve for pile A in Dr=65%

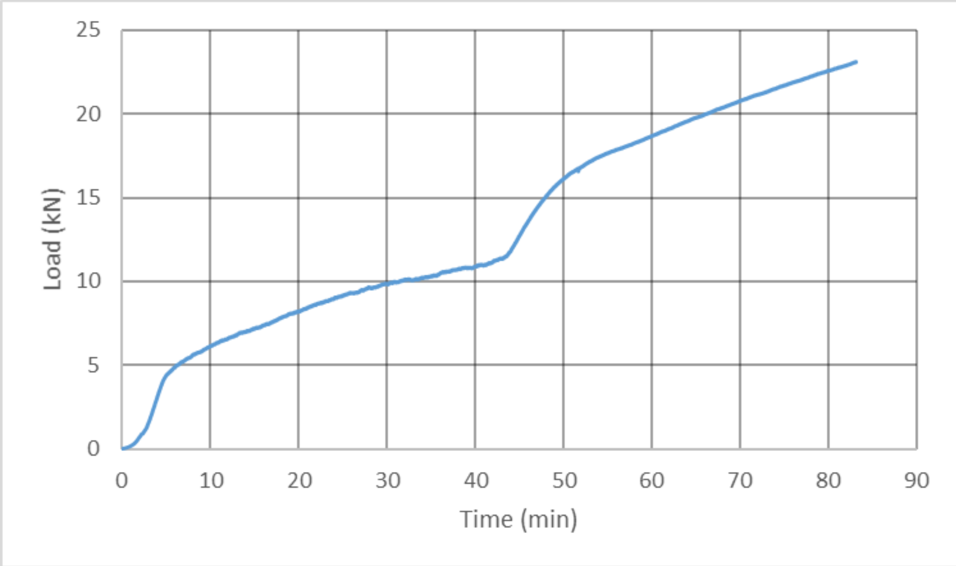

Figure A1.7. Time-Load curve for pile A in Dr=90%

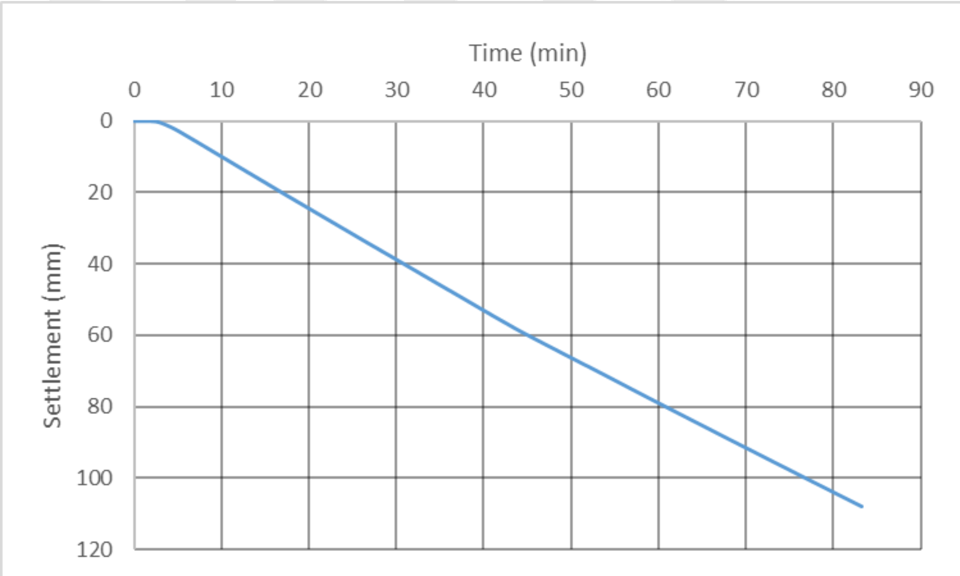

Figure A1.8. Time-Settlement curve for pile A in Dr=90%

APPENDIX- 2: EXPERIMENTAL TIME-LOAD AND TIME-SETTLEMENT CURVES OF PILE B

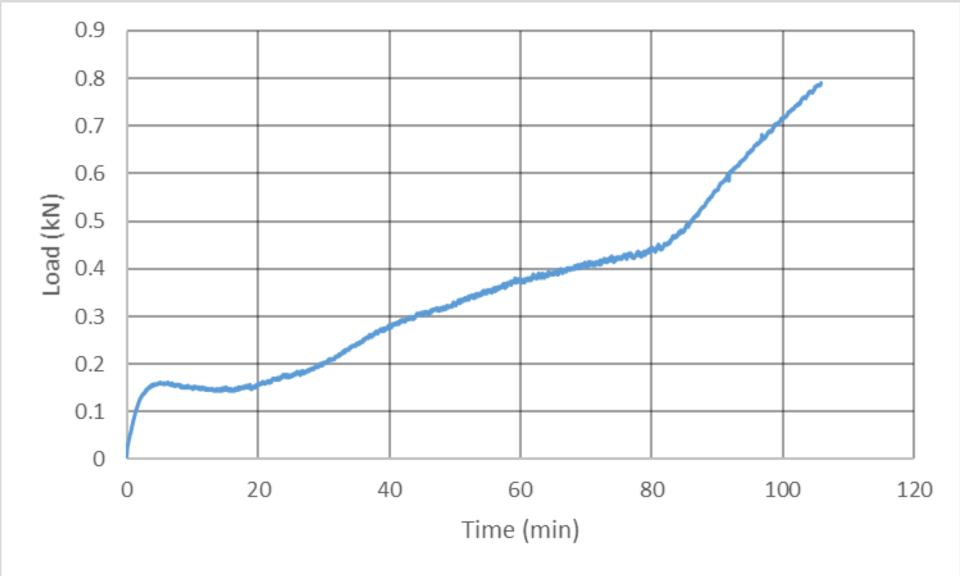

Figure A2.1. Time-Load curve for pile B in Dr=10%

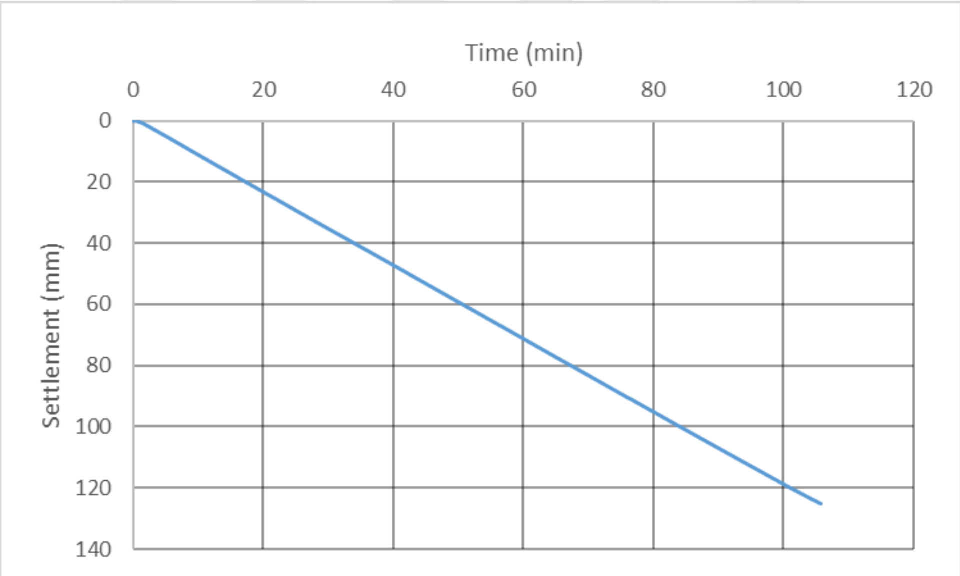

Figure A2.2. Time-Settlement curve for pile B in Dr=10%

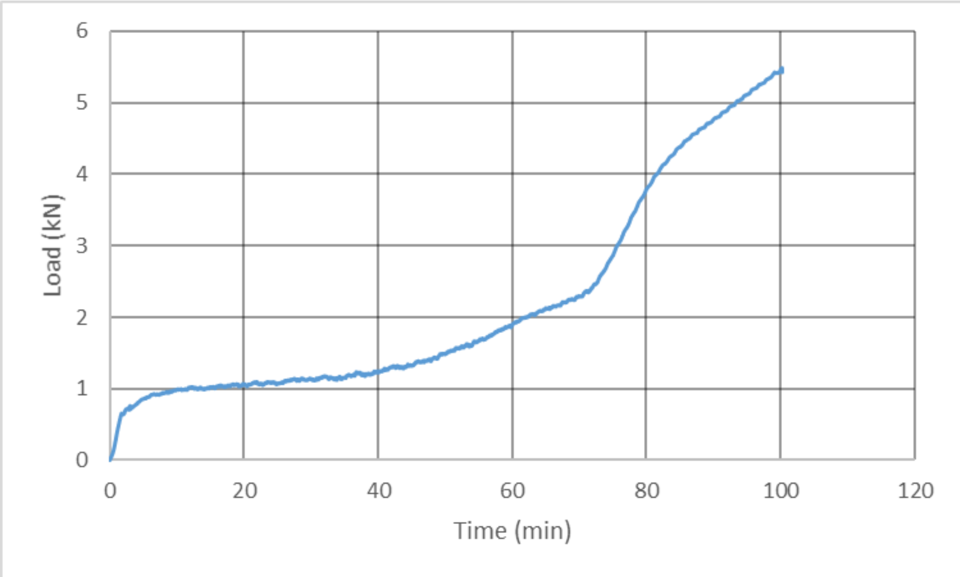

Figure A2.3. Time-Load curve for pile B in Dr=40%

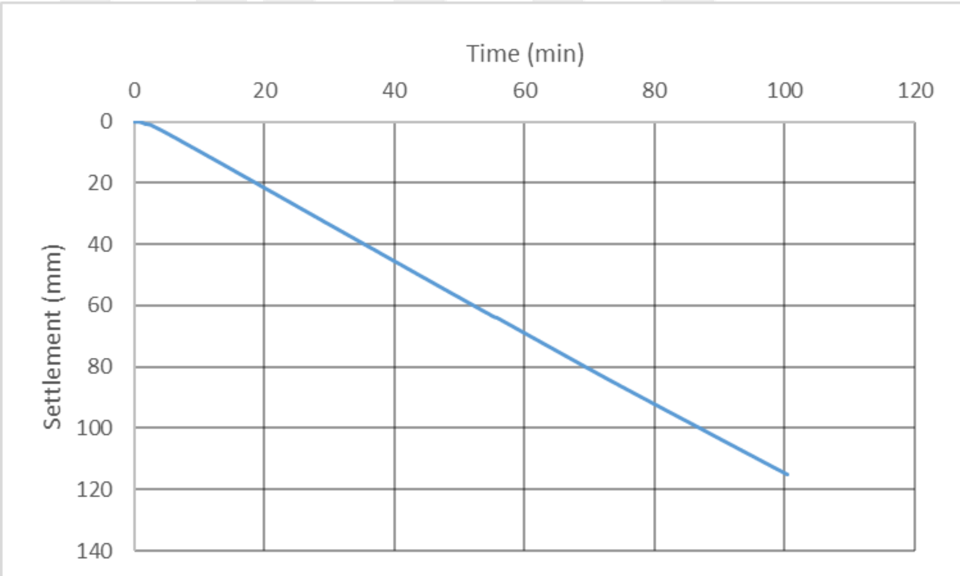

Figure A2.4. Time-Settlement curve for pile B in Dr=40%

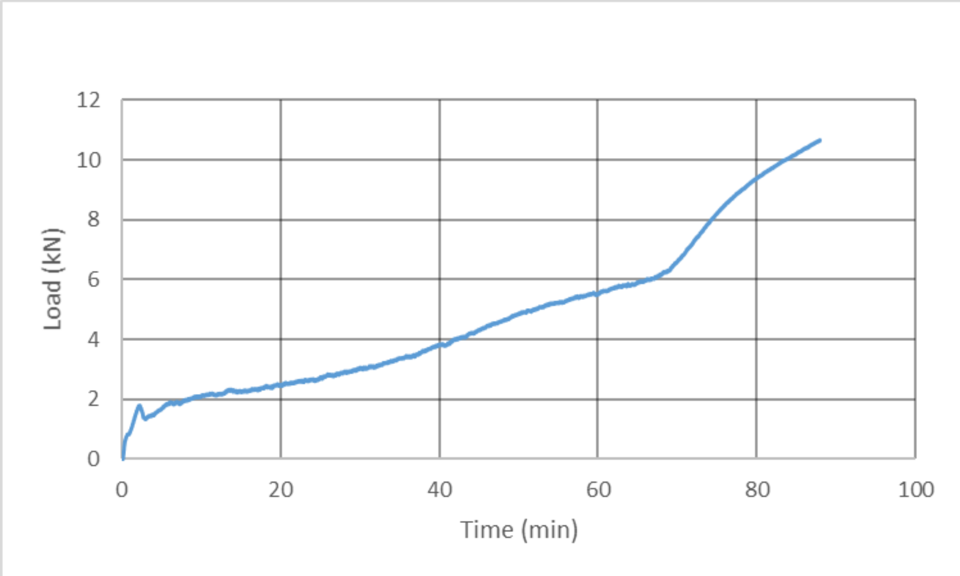

Figure A2.5. Time-Load curve for pile B in Dr=65%

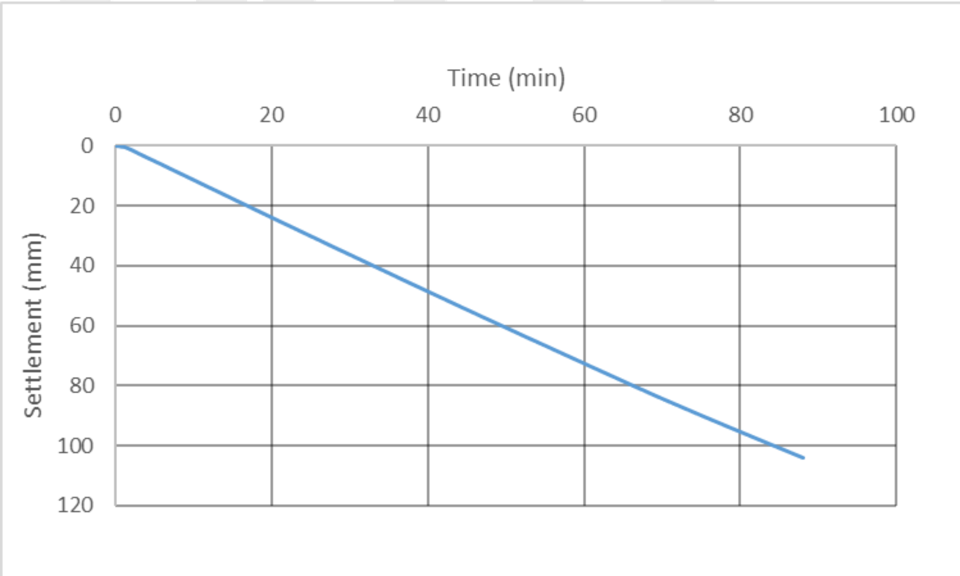

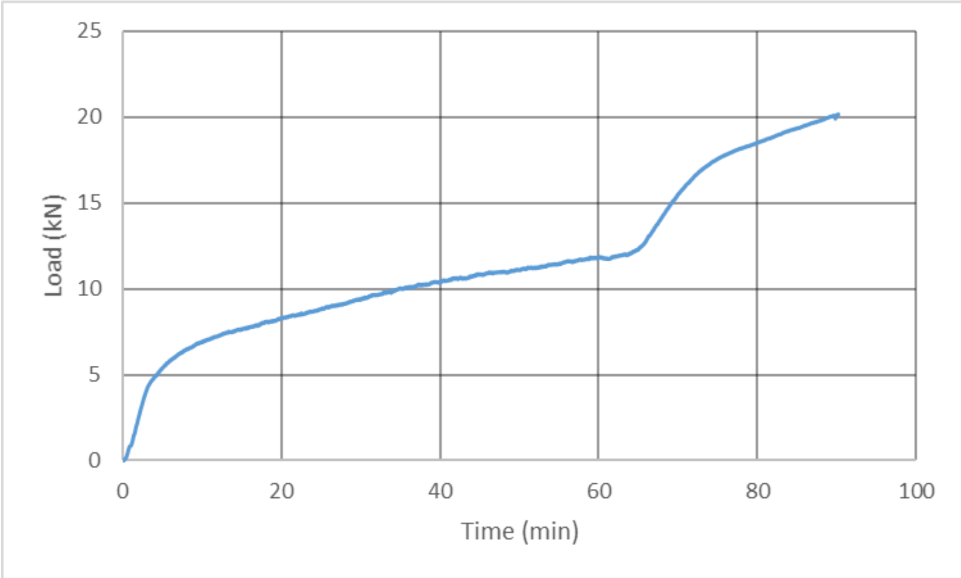

t

curve for pile B in Dr=65%

Figure A2.7. Time-Load curve for pile B in Dr=65%

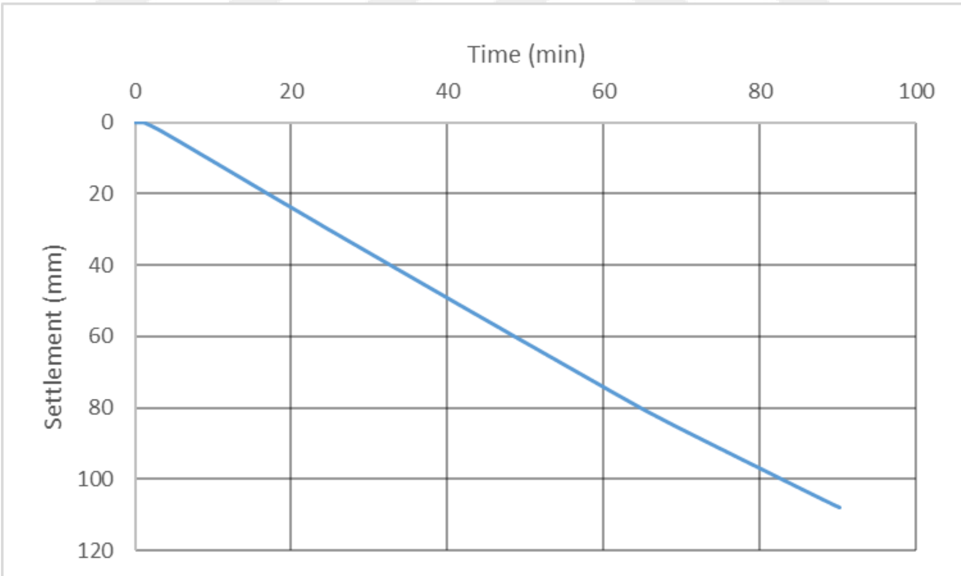

Figure A2.8. Time-Settlement curve for pile B in Dr=90%

CURRICULUM VITAE

Tolaz Salah Hawez

[redacted]

[redacted] [redacted]
[redacted] [redacted]
[redacted] [redacted]
[redacted] [redacted]
[redacted] [redacted]
[redacted] [redacted]

[redacted]

[redacted] [redacted]
[redacted] [redacted]

[redacted]

[redacted] [redacted]

[redacted] [redacted]

[redacted]

- [redacted]
- [redacted]
- [redacted]

[redacted]

- [redacted]
- [redacted]
- [redacted]
- [redacted]